Inorganic Chemistry

Article

pubs.acs.org/IC

Bis-Cyclometalated Iridium(III) Complexes Bearing Ancillary Guanidinate Ligands. Synthesis, Structure, and Highly Efficient Electroluminescence

Virendra Kumar Rai,[†,‡] Masayoshi Nishiura,[†] Masanori Takimoto,[†] Shanshan Zhao,[§] Yu Liu,[§] and Zhaomin Hou*[,†,‡]

[†]Organometallic Chemistry Laboratory and Advanced Catalyst Research Team, RIKEN Advanced Science Institute, 2-1 Hirosawa, Wako, Saitama 351-0198, Japan

[‡]Department of Chemistry, Graduate School of Science and Engineering, Saitama University, 255 Shimo-okubo, Sakura-ku, Saitama 338-8570, Japan

[§]State Key Laboratory of Supramolecular Structure and Materials, Jilin University, Changchun 130012, People's Republic of China

Supporting Information

ABSTRACT: We report the synthesis, structure, and photophysical and electroluminescent (EL) properties of a series of heteroleptic bis(pyridylphenyl)iridium(III) complexes with various ancillary guanidinate ligands. The reaction of the bis(pyridylphenyl)iridium(III) chloride $[(ppy)_2Ir(\mu\text{-}Cl)]_2$ with the lithium salt of various guanidine ligands $Li\{(N^iPr)_2C(NR^1R^2)\}$ at 80 °C gave in 60−80% yield the corresponding heteroleptic bis(pyridylphenyl)/guanidinate iridium(III) complexes having a general formula of $[(ppy)_2Ir\{(N^iPr)_2C(NR^1R^2)\}]$, where NR^1R^2 = NPh_2 (**1**), $N(C_6H_4{}^tBu\text{-}4)_2$ (**2**), carbazolyl (**3**), 3,6-bis(*tert*-butyl)carbazolyl (**4**), $N(C_6H_4)_2S$ (**5**), $N(C_6H_4)_2O$ (**6**), indolyl (**7**), NEt_2 (**8**), N^iPr_2 (**9**), N^iBu_2 (**10**), and $N(SiMe_3)_2$ (**11**). These heteroleptic cyclometalated (C^N) iridium(III) complexes showed intense absorption bands in the UV region assignable to $\pi-\pi^*$ transitions and weaker metal-to-ligand charge-transfer transitions extending to the visible region. These complexes also showed intense emissions at room temperature. Their photoluminescence spectra were influenced to some extent by the ancillary guanidinate ligands, giving λ_{max} values in the range of 528−560 nm with quantum yields (Φ) of 0.16−0.37 and lifetimes of 0.61−1.43 μs. Organic light-emitting diodes were fabricated by the use of these complexes as dopants in various concentrations (5−100%) in a *N*,*N*′-dicarbazolylbiphenyl host. High current efficiency (η_c; up to 137.4 cd/A) and power efficiency (η_p; up to 45.7 lm/W) were observed under appropriate conditions. Their high EL efficiency may result from efficient trapping and radiative relaxation of the excitons formed in the EL process. Because of the steric hindrance of the guanidinate ligands, no significant intermolecular interaction was observed in these complexes, thus leading to the reduction of self-quenching and triplet−triplet annihilation at high currents. The EL emission color could be changed in the range of green to yellow by choosing appropriate guanidinate ligands.

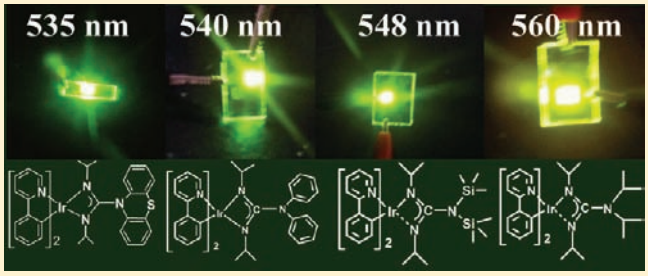

1. INTRODUCTION

Organic light-emitting diodes (OLEDs) have attracted much attention as a promising technology for display systems such as cell phones, flat-panel displays, and solid-state lighting because of their novel properties such as ease of manufacturing, flexibility, fast response, wide-viewing angle, low power consumption, and self-emitting ability.[1] In principle, OLEDs based on triplet-state phosphorescent materials can show much higher emission efficiency than those based on singlet-state fluorescent materials.[1a,2] Among the most promising phosphorescent materials for OLED applications are phosphorescent cyclometalated (C^N) iridium(III) complexes. Because tris(pyridylphenyl)iridium $Ir(ppy)_3$ [ppy = *o*-(2-pyridyl)phenyl; Figure 1, **A**] was first reported to show efficient green electrophosphorescence by Thompson et al. in 2000,[1a] a large number of tris(cyclometalated) iridium(III) complexes with various C^N chelating ligands have been reported to achieve a wide range of emissions for full color display.[2e,h,n] More recently, phosphorescent cyclometalated iridium(III) complexes have also found applications in other fields such as light-emitting electrochemical cells,[2o] luminescence sensitizers,[2p−r] biological labeling,[2s,t] and chemosensors.[2u] Although powerful color tuning was realized by modification of the C^N cyclometalating ligands, unfortunately, synthesis of the homoleptic complexes with the same cyclometalated ligands is often difficult for steric and electronic reasons.[3a] To improve both the synthetic accessibility and electroluminescence (EL) efficiency, various heteroleptic bis-cyclometalated iridium(III) complexes bearing one ancillary monoanionic ligand (Figure 1,

Received: June 7, 2011
Published: December 28, 2011

   dx.doi.org/10.1021/ic201217a | *Inorg. Chem.* 2012, 51, 822−835

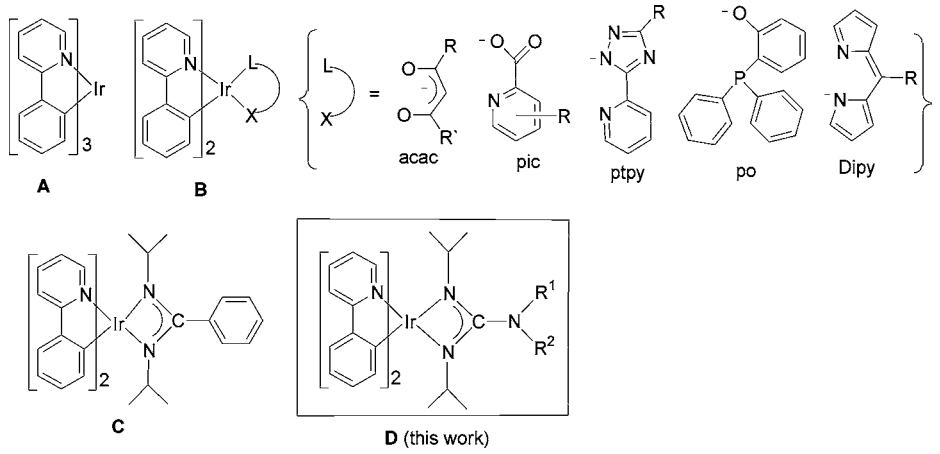

Figure 1. Some typical structure examples of phosphorescent iridium(III) complexes.

Scheme 1. Synthesis of Heteroleptic Bis(2-phenylpyridinato)/Guanidinate Iridium(III) Complexes (1−11)

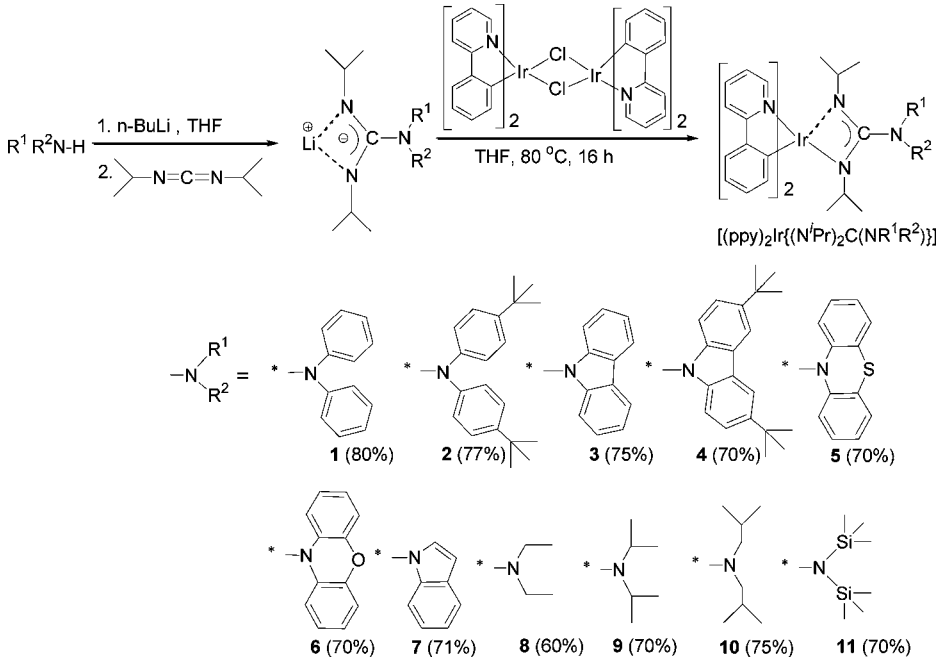

B) have been extensively studied.[2c,3,4] Most of the secondary ancillary ligands reported so far largely relied on acetylacetonate (acac) or nitrogen-containing heterocyclic derivatives. Although many of these heteroleptic iridium(III) complexes showed good photoluminescence (PL), only a few of them were reported to show high EL efficiency,[2c,i,m,3h] because of self-quenching and triplet−triplet (T−T) annihilation problems, which could cause significant efficiency roll-off at higher current density.[5] To overcome these problems, the design and synthesis of more efficient, new phosphorescent iridium(III) complexes is highly desired.

We recently found that amidinate can serve as a useful ancillary ligand for the phosphorescent bis-cyclometalated iridium(III) complexes (Figure 1, **C**), leading to significant improvement of the emitting properties, such as the reduction of self-quenching and insensitivity to doping concentration.[6] During these studies, we became interested in the use of guanidinate units as ancillary ligands for the phosphorescent iridium complexes (Figure 1, **D**). Similar to amidinate, guanidinate can bind transition metals in a chelating fashion, and, moreover, it is more electron-donating than amidinate because it has one more amino group on the central carbon atom and can thus serve as an excellent ancillary ligand to stabilize electron-deficient metal centers and improve the hole-injection (HI) and hole-transport (HT) properties of the resulting complexes.[7−10] However, utilization of guanidinate as an ancillary ligand for phosphorescent metal complexes has not been reported previously.

We report here the synthesis, structural characterization, and photophysical, electrochemical, and EL properties of a novel series of bis(pyridylphenyl)iridium(III) complexes with various ancillary guanidinate ligands (Figure 1, **D**). These phosphorescent complexes can serve as excellent emitting materials for OLEDs, exhibiting both high current efficiency (ca. 116−137 cd/A) and high power efficiency (ca. 33−45 lm/W) under appropriate conditions.

2. RESULTS AND DISCUSSION

2.1. Synthesis and Structural Characterization of Heteroleptic Bis(2-phenylpyridinato)/Guanidinate

dx.doi.org/10.1021/ic201217a | Inorg. Chem. 2012, 51, 822−835

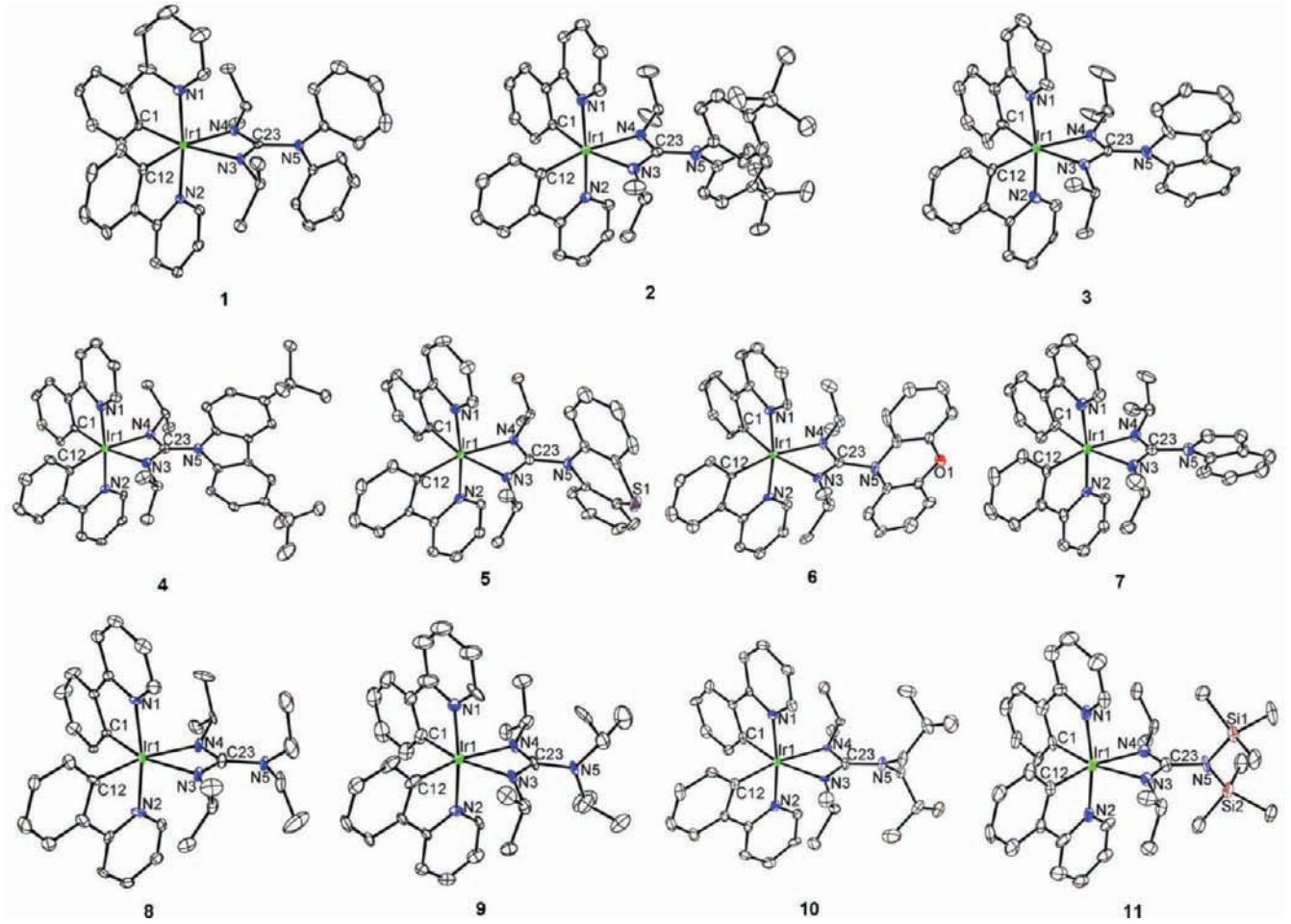

Figure 2. ORTEP drawings of complexes (**1**–**11**) with thermal ellipsoids at 30% probability. Hydrogen atoms are omitted for clarity.

Iridium(III) Complexes [(ppy)$_2$Ir{(N^{i}Pr)$_2$C(NR^{1}R^2)}]. The reaction of the dimeric bis(2-phenylpyridinato)iridium chloride complex [(ppy)$_2$Ir(μ-Cl)]$_2$ with 2 mol equiv of lithium guanidinates Li{(N^{i}Pr)$_2$C(NR^{1}R^2)} prepared in situ from *n*-BuLi with R^{1}R^{2}NH and *N*,*N*′-diisopropylcarbodiimide afforded the corresponding heteroleptic bis(2-phenylpyridinato)/guanidinate iridium(III) complexes [(ppy)$_2$Ir{(N^{i}Pr)$_2$C(NR^{1}R^2)}] (**1**–**11**) in high yields (60–80%), as shown in Scheme 1. These complexes are thermally stable and can be easily sublimed under vacuum. All of these complexes have been fully characterized by ^{1}H and ^{13}C NMR, X-ray diffraction, and microelemental analyses. The ppy ligands in **1**–**11** all showed one set of ^{1}H and ^{13}C NMR signals in tetrahydrofuran (THF)-d_8 or $CDCl_3$ at room temperature, while the guandinate ligands exhibited one set of ^{1}H and ^{13}C NMR signals for its NR^{1}R^2 unit, but two sets for the Me groups in the isopropyl units, indicating that rotation of the ^{i}Pr groups around the ^{i}PrN–C bond in the guanidinate ligands is highly restricted.

The ORTEP drawings of complexes **1**–**11** are shown in Figure 2. Selected bond lengths and angles are summarized in Table 1. The iridium metal center in all of these complexes is bonded to two bidentate ppy ligands and one chelating guanidinate ligand in a distorted octahedral fashion. The coordination geometry of the (ppy)$_2$Ir fragment in **1**–**11** is similar to those in [Ir(ppy)$_2$(acac)] (acac = acetylacetonate)[3a,11] and [(ppy)$_2$Ir(dipba)] (dipba = *N*,*N*′-diisopropylbenzamidinate),[6a] in which the cis-C,C and trans-N,N configurations are retained. The bond lengths of the Ir–C (av. 2.01 Å) and Ir–N(ppy) (av. 2.04 Å) bonds in **1**–**11** are comparable with those in [Ir(ppy)$_2$(acac)] [Ir–C, av. 2.003(9) Å; Ir–N, 2.010(9) Å][3a] and [(ppy)$_2$Ir(dipba)] [Ir–C, av. 2.01 Å; Ir–N, av. 2.04 Å],[6a] respectively. The bond lengths of the Ir–N(guanidinate) bonds (av. 2.19 Å) in **1**–**11** are longer than those of the Ir–N(ppy) bonds but are similar to those of the Ir–N(amidinate) bonds (av. 2.182 Å) in [(ppy)$_2$Ir(dipba)].[6a]

The four core atoms N3, N4, N5, and C23 of the guanidinate unit and the central Ir1 atom in **1**–**11** are placed in a least-squares plane with rather small deviation (0.004–0.0481 Å; Table 1). To see possible influences of the R^1 and R^2 substituents at the N5 atom on the structure of the complexes, the dihedral angles of N(3,4)–C23–N5–R(1,2) were examined. It was found that the R^1 and R^2 substituents at the N5 atom showed significant influence of these dihedral angles. The average value (55.2°) of the two smallest dihedral angles among N(3,4)–C23–N5–R(1,2) in complex **2**, which has sterically demanding R^1 = R^2 = C$_6$H$_4$^{t}Bu-*p* substituents, is significantly smaller than that (64.9°) in the analogous complex **1** having unsubstituted phenyl groups. In contrast, such an average dihedral angle (79.5°) in the *tert*-butylcarbazolyl-substituted complex **4** is larger than that (62.9°) in the analogous complex **3** having unsubstituted carbazolyl units. The average dihedral angle in a complex having an indenyl substituent (**7**; 55.8°) is smaller than that having phenothiazine **5** (76.3°) or phenoxazine **6** (76.3°) substituents. Among complexes having

dx.doi.org/10.1021/ic201217a | *Inorg. Chem.* 2012, 51, 822–835

Table 1. Selected Bond Distances (Å) and Angles (deg) of 1−11

	1	2	3	4	5	6	7	8	9	10	11
Ir1−C1	2.018(6)	1.995(4)	2.019(10)	1.997(5)	2.012(6)	2.003(9)	1.992(8)	1.955(13)	2.023(11)	2.009(5)	2.043(14)
Ir1−C12	2.002(7)	2.006(4)	2.007(10)	1.996(4)	2.008(6)	2.027(9)	2.028(8)	2.028(13)	1.995(12)	1.999(5)	2.005(13)
Ir1−N1	2.043(6)	2.032(3)	2.067(8)	2.023(4)	2.039(5)	2.043(7)	2.042(6)	2.048(9)	2.039(9)	2.037(4)	2.020(11)
Ir1−N2	2.033(5)	2.030(3)	2.045(8)	2.022(4)	2.037(5)	2.054(7)	2.045(6)	2.036(10)	2.024(8)	2.040(4)	2.004(11)
Ir1−N3	2.186(5)	2.182(3)	2.196(8)	2.172(4)	2.195(5)	2.203(7)	2.216(7)	2.183(10)	2.198(8)	2.176(4)	2.214(11)
Ir1−N4	2.193(5)	2.202(3)	2.195(8)	2.190(3)	2.189(5)	2.192(7)	2.196(6)	2.156(11)	2.190(8)	2.181(4)	2.189(12)
C1−Ir1−N1	81.2(2)	79.95(14)	79.1(4)	79.38(18)	80.1(2)	80.4(3)	80.3(3)	79.2(5)	80.9(5)	80.52(19)	80.2(5)
C1−Ir1−N3	167.3(2)	165.83(12)	166.0(3)	166.60(15)	166.4(2)	165.8(3)	165.8(3)	162.2(5)	164.8(4)	166.67(17)	165.3(5)
C1−Ir1−N4	107.4(2)	106.25(13)	106.4(3)	107.33(14)	106.7(2)	105.3(3)	106.2(3)	102.5(5)	105.9(4)	107.49(17)	106.5(5)
C12−Ir1−C1	86.8(3)	87.51(14)	88.6(4)	88.93(19)	87.4(3)	89.2(3)	86.8(3)	90.5(5)	88.1(5)	84.91(19)	88.6(5)
C12−Ir1−N2	80.4(3)	80.49(14)	80.3(4)	80.15(16)	80.4(2)	80.3(3)	80.7(3)	80.9(5)	80.9(4)	80.57(18)	80.5(5)
C12−Ir1−N3	105.7(2)	106.10(13)	104.6(3)	103.81(18)	106.0(2)	104.9(3)	106.9(3)	106.8(5)	107.0(4)	107.61(17)	105.5(5)
N2−Ir1−N1	173.8(2)	175.51(12)	172.6(3)	174.62(16)	173.0(2)	171.2(3)	174.0(3)	170.8(4)	174.0(3)	173.51(16)	170.7(4)
N3−Ir1−N4	60.36(19)	60.42(11)	60.7(3)	60.21(13)	60.1(2)	60.8(3)	60.5(3)	60.6(4)	59.1(3)	60.38(14)	59.8(4)
Ir1−N_2CN planarity[a]	0.0127	0.0053	0.0088	0.0063	0.0052	0.0192	0.0325	0.0251	0.0481	0.0063	0.0040
N3−C23−N5−R1[b]	60.0(9)	55.3(5)	66.0(14)	74.8(6)	71.0(8)	104(1)[c]	59(1)	53(2)	88(1)	41.9(7)	67(2)
N4−C23−N5−R2[b]	69.8(8)	55.1(5)	59.7(15)	84.1(6)	81.6(8)	78(1)	53(1)	54(2)	92(1)[d]	49.2(7)	70.0(2)

[a]Deviation (Å) from the Ir1−N3−N4−C23−N5 least-squares plane. [b]The smallest dihedral angle among N(3,4)−C23−N5−R(1,2), unless otherwise noted. See also Figure 2 and Scheme 1. [c]The dihedral angle of N4−C23−N5−R1 [75(1)°] is smaller. [d]The dihedral angle of N3−C23−N5−R2 [85(1)°] is smaller.

dx.doi.org/10.1021/ic201217a | Inorg. Chem. 2012, 51, 822−835

Table 2. Photophysical Data of Complexes 1−11

iridium(III) complex	λ_{abs} ($\varepsilon \times 10^3$ M^{-1} cm^{-1})	emission λ_{max} (nm) in CH_2Cl_2	emission λ_{max} (nm) in the solid state	τ (μs)[a]	Φ_{PL}[b]	k_r (10^5 s^{-1})[c]	k_{nr} (10^5 s^{-1})[d]
1	262 (20.4), 352 (2.5), 402 (1.4), 465 (0.39), 505 (0.23).	535	540	1.41	0.36	2.5	4.5
2	265 (12.3), 353 (1.4), 402 (1.2), 470 (0.30), 506 (0.21).	535	540	1.42	0.20	1.4	5.6
3	261 (30.1), 340 (5.5), 396 (3.1), 462 (1.0), 499 (0.77).	528	528	1.09	0.27	2.4	6.6
4	264 (14.3), 290 (10.4), 344 (3.0), 395 (1.6), 465 (0.79), 500 (0.67).	530	530	1.35	0.21	1.5	5.8
5	266 (40.1), 345 (8.1), 397 (6.2), 470 (2.2), 497 (1.7).	530	535	0.28, 0.70	0.22		
6	260 (14.1), 290 (11.5), 352 (2.4), 398 (1.9), 470 (0.89), 496 (0.76).	528	532	0.61	0.21	3.4	12.9
7	260 (36.4), 350 (4.6), 393 (5.0), 470 (1.4), 496 (1.0).	532	532	1.24	0.37	2.9	5.0
8	260 (41.6), 357 (7.4), 402 (8.5), 480 (2.2), 514 (1.8).	548	558	1.34	0.16	1.1	6.2
9	261 (30.7), 356 (4.0), 405 (3.8), 472 (1.4), 508 (1.1).	548	560	1.38	0.16	1.1	6.0
10	286 (30.6), 355 (9.5), 406 (11.2), 480 (2.7), 510 (2.3).	548	558	1.28	0.17	1.3	6.4
11	285 (38.9), 355 (8.6), 408 (10.5), 480 (2.6), 512 (2.2).	538	546	1.43	0.18	1.2	5.7

[a]Phosphorescent lifetime measured in THF at room temperature. [b]PL quantum yield in THF. [c]Radiative decay rate $k_r = \Phi/\tau$. [d]Nonradiative decay rate $k_{nr} = (1 - \Phi)/\tau$. The experimental error range is ±1% for lifetimes and ±5% for quantum yields.

alkyl R^1 and R^2 groups, the isopropyl-containing complex **9** exhibited the biggest dihedral angle (86.3°), in which the isopropyl groups are almost perpendicular to the plane formed by the Ir1, N3, N4, N5, and C23 atoms. No obvious intermolecular interaction was observed in any of these complexes.

2.2. Photophysical Properties. Complexes **1−11** showed almost the same absorption spectra in the range of 250−550 nm (Table 2 and Figure 3). Intense absorption bands were

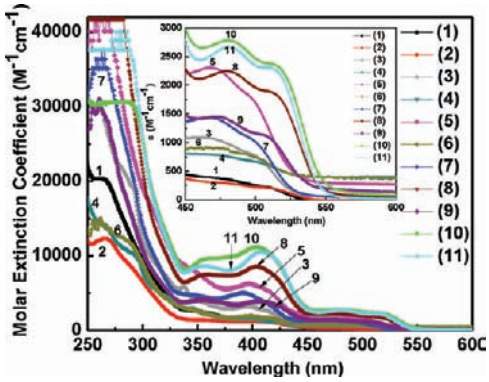

Figure 3. Absorption spectra of complexes **1−11** in CH_2Cl_2 solution.

observed in the ultraviolet region between 250 and 350 nm, assignable to spin-allowed $^1(\pi-\pi^*)$ transitions of ppy and other aromatic moieties. The absorption bands observed at lower energies extending into the region of 350−450 nm can also be assigned to spin-allowed $^1(\pi-\pi^*)$ transitions of ppy and other aromatic moieties (Figure S2 in the Supporting Information), along with minor contribution from spin-allowed metal-to-ligand charge transfer (MLCT). These MLCT bands are attributed to an effective mixing of charge-transfer transitions with higher-lying spin-allowed transitions on the cyclometalated ligands,[12] which is facilitated by strong spin−orbit coupling with the iridium(III) center. The lower-energy weak shoulder peaks extending into the 450−550 nm region are mainly derived from a spin-forbidden ligand-centered $^3(\pi-\pi^*)$ transition as well as some ^{3}MLCT contribution, due to the substantial reduction in the absorption extinction coefficient (Figure 3, inset). The absorption bands of **1−11** for the singlet (^{1}MLCT) and triplet (^{3}MLCT) transitions are similar to those reported for $[Ir(ppy)_2(bpy)]^+$ (bpy = bipyridine),[13] $[Ir(ppy)_2(acac)]$,[2c] and $[(ppy)_2Ir(dipba)]$.[6a] In complexes with guanidinate ligands having aliphatic R substituents (**8−11**), the MLCT transitions appeared distinctively above 500 nm. This suggests substantial mixing of spin-forbidden ^{3}MLCT and higher-lying ^{1}MLCT transitions by spin−orbit coupling of the iridium metal,[14] probably because of the electron-donating effect of the aliphatic substituents.

The PL spectra of **1−11** in a degassed dichloromethane solution at room temperature showed intensive emissions at 528−548 nm under UV-light irradiation at 350 nm (Figure 4

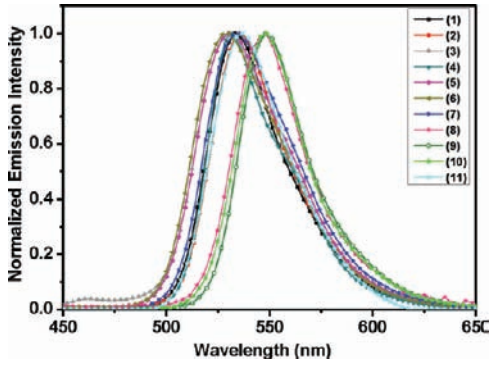

Figure 4. PL spectra of complexes **1−11** in CH_2Cl_2 solutions.

and Table 2). The excited states for emission of all of the complexes **1−11** have been identified as ligand-centered transition $[LC^3(\pi-\pi^*)(ppy)]$ with significant MLCT $[d\pi(Ir)-\pi^*(ppy)]$ character. Complexes **3**, **4**, and **7** showed almost identical maximum emission both in the solid state and in solution, implying the absence of any appreciable aggregates in the solid state. However, other complexes (**1**, **2**, **5**, **6**, and **8−11**) showed ca. 5−12 nm red shifts in the PL spectrum in the solid state compared to that in solution (Table 2) probably because of the formation of excimers in the solid state.

The complexes with guanidinate ligands having aromatic NR^1R^2 moieties showed moderate PL quantum yields (**1−11**; Φ = 0.16−0.37; Table 2), which are generally comparable to those of the acac- or amidinate-supported analogues such as

dx.doi.org/10.1021/ic201217a | Inorg. Chem. 2012, 51, 822−835

$[Ir(ppy)_2(acac)]$ (Φ = 0.25)[4j] and $[(ppy)_2Ir(dipba)]$ (Φ = 0.30).[6a]

The phosphorescence lifetimes of complexes **1**−**11** in THF at room temperature are in the range of 0.61−1.43 μs (Table 2), which are slightly shorter than that of the acac-coordinated complex $[Ir(ppy)_2(acac)]$ (1.6 μs),[3a] suggesting that there is spin−orbit coupling leading to intersystem crossing from the singlet to triplet state in the guanidinate complexes.[2c] The relatively short phosphorescence lifetime may allow the design and fabrication of highly efficient OLEDs based on light-energy harvesting from the triplet exciton, because a short phosphorescence lifetime could decrease the detrimental T−T annihilation process. The radiative decay rates (k_r) of the guanidinate complexes **1**−**11** range from 1.1×10^5 s^{-1} to 3.4×10^5 s^{-1} and are similar to that of the acac analogue $[Ir(ppy)_2(acac)]$ (2.1×10^5 s^{-1}).[3a]

2.3. Cyclic Voltammetry and Density Functional Theory (DFT) Studies. The redox potentials of complexes **1**−**11** measured by cyclic voltammetry are summarized in Table 3. The cyclic voltammograms of **5** and **8** are shown in Figure 5 as representative examples of complexes having aromatic NR^1R^2 moieties and aliphatic substituents, respectively. All of these guanidinate complexes, except **7**, showed two oxidation waves (ranging from +0.21 to +0.47 V and from +0.70 to +1.12 V, respectively) and two reduction peaks (ranging from −1.43 to −1.28 V and from −2.75 to −2.55 V, respectively) in an acetonitrile solution, in contrast with the acac analogue $[Ir(ppy)_2(acac)]$, which showed only one oxidation peak (+0.42 V) and one reduction peak (−2.52 V).[4j,k] Complex **7** exhibited one oxidation (+0.44 V) and two reduction peaks (−1.38 and −2.62 V). The first oxidation waves of the complexes with guanidinate ligands having aromatic NR^1R^2 moieties (**1**−**6**) appeared in a relatively narrow range of +0.40 to +0.47 V, which are higher than those of the complexes having aliphatic NR^1R^2 groups (**8**−**11**; +0.21 to +0.24 V). The second oxidation waves of the aromatic complexes **1**−**6** (ranging from +0.70 to +0.82 V) are, however, lower than those of the aliphatic complexes **8**−**11** (ranging from +1.06 to +1.12 V). It was previously reported that the oxidation process in (2-pyridylphenyl)iridium(III) complexes usually takes place at the Ir−phenyl moiety, and the reduction occurs mainly at the pyridine unit of the ppy ligands.[13,15] Therefore, the first oxidation peaks of complexes **1**−**11** are attributable to oxidation of the Ir−ppy moiety, and the second oxidation peaks could result from oxidation of the guanidinate unit $\{(N^iPr)_2C(NR^1R^2)\}$.[10d,16]

Table 3. Electrochemical Data of Complexes 1−11[a]

iridium(III) complex	E^{ox} (V)	E^{red} (V)	bandgap E_g (eV)	HOMO (eV)	LUMO (eV)
1	+0.40, +0.74	−1.42, −2.60	2.30	−4.98	−2.68
2	+0.47, +0.77	−1.42, −2.60	2.30	−5.05	−2.75
3	+0.46, +0.74	−1.38, −2.58	2.35	−5.04	−2.69
4	+0.42, +0.70	−1.35, −2.55	2.35	−5.00	−2.65
5	+0.45, +0.75	−1.42, −2.58	2.33	−5.03	−2.70
6	+0.47, +0.82	−1.40, −2.60	2.35	−5.05	−2.70
7	+0.44	−1.38, −2.62	2.33	−5.02	−2.69
8	+0.21, +1.12	−1.35, −2.70	2.26	−4.79	−2.53
9	+0.21, +1.10	−1.28, −2.73	2.25	−4.79	−2.54
10	+0.21, +1.06	−1.33, −2.75	2.26	−4.79	−2.53
11	+0.24, +1.12	−1.43, −2.70	2.30	−4.82	−2.52

[a]0.1 M tetrabutylammonium perchlorate, versus Ag/Ag^+ couple, scan rate 100 mV/s. HOMO = $E_{ox} - E_{ox(Fc/Fc^+)}$ (4.8 eV). The ferrocene has an E_{ox} at 0.22 V relative to Ag/Ag^+. LUMO = HOMO + E_g. The bandgap (E_g) was estimated from the onset wavelength of the optical absorption edge.

On the basis of the first oxidation potential and optical absorption edge of the UV−vis spectra, the highest occupied molecular orbital (HOMO), the lowest unoccupied molecular orbital (LUMO), and the energy gap (E_g) were calculated.[17] The HOMO levels of **1**−**11** are located in the range of −5.05 to −4.79 eV, which are similar to that of the amidinate analogue $[(ppy)_2Ir(dipba)]$ (−4.78 eV) complex[6a] but higher than those of the acac analogue $[Ir(ppy)_2(acac)]$ (−5.60 eV)[2i] and the homoleptic complex $[Ir(ppy)_3]$ (−5.40 eV).[2k] A higher HOMO energy level usually leads to better HI and HT ability in OLEDs, and, therefore, the guanidinate-ligated complexes **1**−**11** may serve as bifunctional phosphorescent emitters. The HOMO−LUMO energy gaps (E_g = 2.25−2.26 eV) of complexes **8**−**10** having alkyl NR^1R^2 substituents are somewhat smaller than those (E_g = 2.30−2.35 eV) of the complexes having aromatic NR^1R^2 moieties (**1**−**7**) or silyl substituents $N(SiMe_3)_2$ (**11**), consistent with their maximum emission wavelengths (Figure 4).

The reduction peaks of **1**−**11** ranging from −1.28 to −2.75 V could be assigned to reduction of the pyridyl ring of the ppy

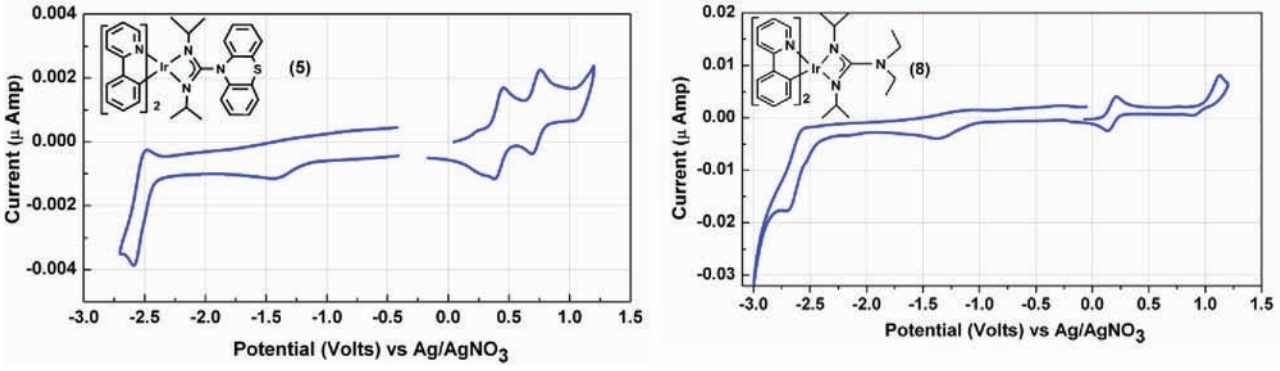

Figure 5. Cyclic voltammograms of **5** (left) and **8** (right).

dx.doi.org/10.1021/ic201217a | Inorg. Chem. 2012, 51, 822−835

ligands as reported for other iridium(III) complexes bearing ppy ligands.[2g] The reduction potentials of **1**−**11** each fall in a relatively narrow range (Table 3), suggesting that the LUMO energy levels in these complexes are not significantly affected by the NR^1R^2 substituents.

To ascertain the influence of the guanidinate ancillary ligand [{$(N^iPr)_2C(NR^1R^2)$}] on the luminescence properties of the iridium(III) complexes, the DFT studies of complex **9** were carried out as a representative example. The contour plots of HOMO and LUMO of **9** are shown in Figure 6. The HOMO

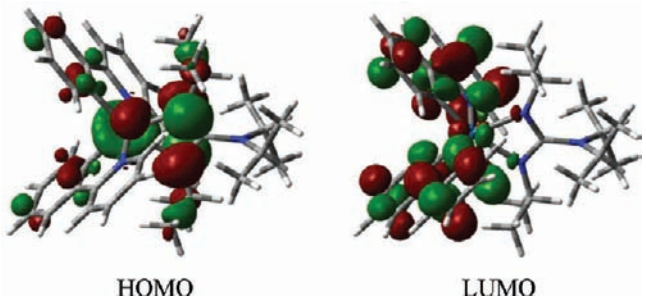

Figure 6. Contour plots of HOMO and LUMO in complex **9** from DFT calculations.

of **9** consists principally of a mixture of the nitrogen atoms of the guanidinate ancillary ligand {$(N^iPr)_2CN(^iPr)_2$} (56.7%) and the d orbitals of the iridium atom (26.4%). This is similar to that of the amidinate analogue [$(ppy)_2Ir(dipba)$],[6a] in which the contributions of the amidinate ligand and the d orbitals of the iridium atom were 49.1% and 29.6%, respectively, but different from those of $(ppy)_2Ir(acac)$, which are distributed on the π orbitals of the ppy ligands in addition to the Ir d orbitals. These results can be ascribed, in part, to the π-bonding ability of the guanidinate ligand being stronger than that of the acac ligand.[15b] However, the LUMO of complex **9** is located largely on the ppy ligand (Figure 6), which is similar to those of the amidinate complex [$(ppy)_2Ir(dipba)$][6a] and the analogous complexes $Ir(ppy)_3$ and $(ppy)_2Ir(acac)$.[15b]

2.4. EL Properties. To examine the electrophosphorescence properties of the guanidinate complexes **1**−**11**, a series of devices were fabricated with the same structure of indium−tin oxide (ITO)/NPB (300 Å)/emitter (250 Å)/BCP (60 Å)/Alq_3 (200 Å)/LiF (10 Å)/Al (1000 Å), where NPB (4,4-bis[*N*-(1-naphthyl)-*N*-phenylamino]biphenyl) serves as a hole-transporting layer (HTL), BCP (2,9-dimethyl-4,7-diphenyl-1,10-phenanthroline) serves as a hole-blocking layer (HBL), and Alq_3 [tris(8-hydroxyquinoline)aluminum] serves as an electron-transporting layer (ETL). The EL properties were examined at various doping levels (5, 10, 20, and 100 wt %) in the *N*,*N*′-dicarbazolylbiphenyl (CBP) host matrix to investigate the influence of the doping concentration on the EL efficiency and to identify the optimum emitter−host ratio. For comparison, the EL properties of complexes **1**−**11** at 5 wt % doping concentration are summarized in Table 4 and the EL spectra are shown in Figure 7.

Complexes **1**−**7**, which have aromatic NR^1R^2 moieties, showed bright-green emissions (λ_{max} = 528−540 nm). Complexes **8**−**11** having aliphatic NR^1R^2 substituents emitted yellowish-green light with λ_{max} = 548−560 nm, which are slightly red-shifted (ca.10−30 nm) from those of **1**−**7**. The emission spectra of all complexes were independent of the doping concentration and resembled their PL spectra,

Table 4. EL Characteristics of OLEDs with 5 wt % Iridium(III) Complexes in the CBP Host

iridium(III) complex	voltage (turn-on)	L_{max} (cd/m^2), voltage	$\eta_{c,max}$ (cd/A)	$\eta_{p,max}$ (lm/W)	λ_{max} (nm)	CIE coordinates
1	3.5	42 581, 16 V	125.0	43.6	540	X = 0.42, Y = 0.56
2	4.0	19 466, 16 V	38.8	8.7	540	X = 0.38, Y = 0.60
3	4.0	25 670, 16 V	75.0	28.0	528	X = 0.36, Y = 0.60
4	4.0	18 560, 16 V	42.0	14.0	530	X = 0.36, Y = 0.58
5	4.0	34 200, 16 V	118.0	42.2	535	X = 0.38, Y = 0.58
6	3.5	19 472, 16 V	48.7	13.7	532	X = 0.37, Y = 0.59
7	4.0	16 749, 16 V	59.1	38.3	532	X = 0.36, Y = 0.58
8	4.0	45 743, 16 V	47.0	16.4	558	X = 0.47, Y = 0.52
9	4.0	42 638, 15 V	116.5	45.7	560	X = 0.46, Y = 0.52
10	4.0	34 698, 16 V	137.4	39.2	558	X = 0.48, Y = 0.51
11	4.0	30 343, 16 V	115.7	25.9	548	X = 0.43, Y = 0.55

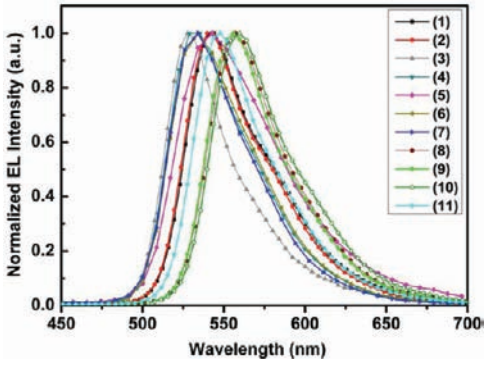

Figure 7. EL spectra of complexes **1**−**11**.

respectively (Figures 4 and 7), suggesting that EL should originate from the triplet states of the iridium-based phosphors. No obvious emission from CBP or Alq_3 was observed in any device even at high current densities, indicating that an efficient energy transfer from the host exciton to the phosphor molecule takes place upon electrical excitation and BCP works effectively as a HBL.

Significant influence of the NR^1R^2 units on the EL efficiencies was observed. Complex **1** having a simple diphenylamino group showed much higher luminance intensity (L_{max} = 42581 cd/m^2), current efficiency (η_c = 125.0 cd/A), and power efficiency (η_p = 43.6 lm/W) than those of the analogous complex **2** having the ^{t}Bu-substituted diphenylamino group (L_{max} = 19466 cd/m^2, η_c = 38.8 cd/A, and η_p = 8.7 lm/W), although the maximum emission wavelengths of the two complexes are the same (Table 4). Similarly, the unsubstituted carbazolyl-containing complex **3** showed a much better performance (L_{max} = 25670 cd/m^2, η_c = 75.0 cd/A, and η_p = 28.0 lm/W) than that of the ^{t}Bu-substituted analogue **4** (L_{max} = 18560 cd/m^2, η_c= 42.0 cd/A, and η_p= 14.0 lm/W). The phenothiazine-containing complex **5** showed higher luminance intensity (L_{max} = 34 200 cd/m^2), current efficiency (η_c = 118.0 cd/A), and power efficiency (η_p = 42.2 lm/W) than those of

dx.doi.org/10.1021/ic201217a | *Inorg. Chem.* 2012, 51, 822−835

the analogous phenoxazine-containing complex **6** (L_{max} = 19 472 cd/m^2, η_c = 48.7 cd/A, and η_p = 13.7 lm/W), showing that a sulfur bridge between the two phenyl rings is more effective than an oxygen linker. An indenyl moiety (**7**) is somewhat less effective compared to a carbazolyl group (**3**) in terms of maximum luminance intensity and maximum current efficiency (Table 4). In the case of complexes having alkyl R substituents, the ^{i}Pr- and CH$_2{}^i$Pr-containing complexes **9** and **10** showed higher current efficiency (**9**, η_c = 116.5 cd/A; **10**, η_c = 137.4 cd/A) and power efficiency (**9**, η_p = 45.7 lm/W; **10**, η_p = 39.2 lm/W) than those of the analogous complex **8** having less sterically demanding ethyl substituents (η_c = 47.0 cd/A; η_p = 16.4 lm/W). The maximum current efficiency of the Me$_3$Si-substituted complex **11** (η_c = 115.7 cd/A) is comparable with that of **9**, but its maximum power efficiency (η_p = 25.9 lm/W) is lower than that of **9**.

Many of the guanidinate complexes, such as **1**, **5**, **9**, and **10**, showed both higher current efficiencies (η_c = 118.0−137.4 cd/A) and power efficiencies (η_p = 39.2−45.7 lm/W) than the analogous complexes bearing other ancillary ligands, such as [(ppy)$_2$Ir(dipba)] (η_c = 68 cd/A; η_p = 32.5 lm/W),[6a] [Ir(ppy)$_2$(acac)] (η_p = 38 lm/W),[2c] and [Ir(ppy)$_3$] (η_p = 31 lm/W),[2j] reflecting the higher electron-donating property of the guanidinate ligands, which promote HI/HT to enhance the EL efficiency.[18−21]

Figure 8 shows the current density−voltage−luminance (J−V−L) characteristics of the device with 5 wt % doping

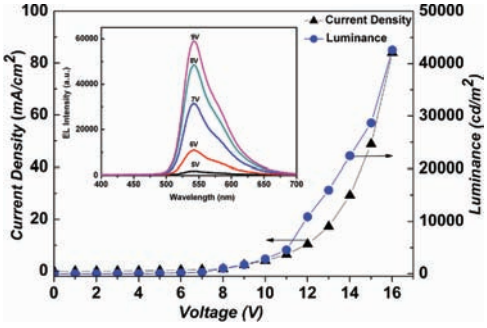

Figure 8. Current density and luminance characteristics as a function of the voltage for a device with 5 wt % **1** in the CBP host. Inset: EL spectra at different voltages.

concentration of **1**. A turn-on voltage was observed at 3.5 V. The maximum brightness (L_{max}) reached as high as 42 581 cd/m^2 at 16 V. The maximum emission wavelength remained almost constant at the voltage range of 3.5−16 V.

The current efficiency and power efficiency versus current density of devices with different doping concentrations of **1** are shown in Figure 9. It is particularly noteworthy that the current efficiency (up to 125.0 cd/A) and power efficiency (up to 43.6 lm/W) of these devices are relatively similar at a wide range of current density or electric voltage despite different doping concentrations (5%, 10%, 20%, and 100%). At a current density of 9.2 mA/cm^2, the nondoped device (100%) showed a maximum current efficiency of 111.2 cd/A and a maximum power efficiency of 29.8 lm/W, which are even slightly higher than those of the doped devices at the same current density (Figure 9). These results clearly demonstrate that the EL efficiency of complex **1** is not critically sensitive to the doping concentration, unlike most phosphorescent materials reported previously. Similar doping concentration insensitivity was also

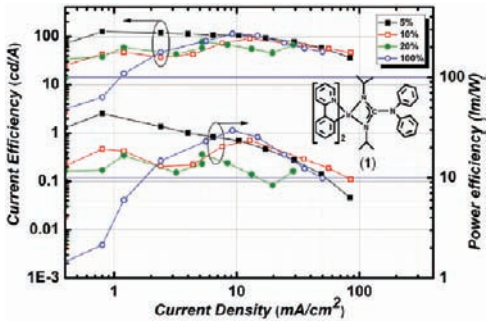

Figure 9. Current (left) and power (right) efficiencies of devices with different doping concentrations of complex **1**.

observed in our recent studies on benzamidinate-ligated [(ĈN)$_2$Ir(dipba)] complexes.[6] Such insensitivity of the EL efficiency to the doping concentration would make device fabrication much easier and more reproducible because a sophisticated control of the emitter doping concentration to a narrow range in a host matrix is not required. These results demonstrate that amidinate or guanidinate chelate moieties could generally serve as excellent ancillary ligands for phosphorescent iridium(III) complexes because of their ability to prevent or reduce self-quenching caused by T−T annihilation. Obviously, guanidinate is superior to amidinate in terms of its electron-donating ability and ease of substituent modification.

Similar to **1**, high EL efficiency (η_c up to 118.0 cd/A; η_p up to 42.2 lm/W) and insensitivity to the doping concentration were also observed in the case of **5** (Table 4 and Figure 10).

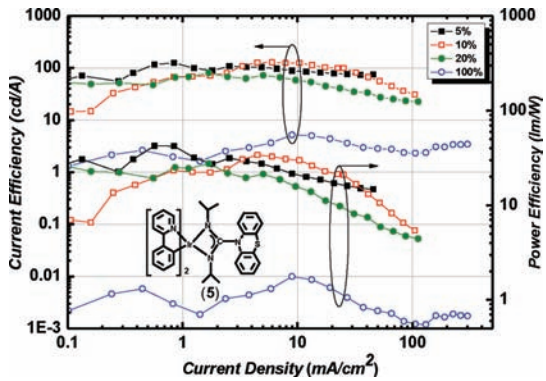

Figure 10. Current (left) and power (right) efficiencies of devices with different doping concentrations of complex **5**.

Devices with 5, 10, and 20 wt % of complex **5** showed rather similar EL properties at a wide range of current densities, although the nondoped device showed a much poorer performance (Figure 10). The maximum power efficiencies for 10 and 20 wt % based devices were around 32.8 and 27.5 lm/W, respectively (Figure 10). The device performance deceases at a higher doping concentration of 100% (nondoped).

As a representative example of iridium guanidinate complexes having aliphatic NR^{1}R^2 moieties, the EL properties of devices based on complex **9** at various doping levels are shown in Figure 11. At the current density range of 20−70 mA/cm^2, the current efficiency of the device with 5% doping concentration is very close to that with 10% doping concentration. At current densities of 1−20 mA/cm^2,

dx.doi.org/10.1021/ic201217a | Inorg. Chem. 2012, 51, 822−835

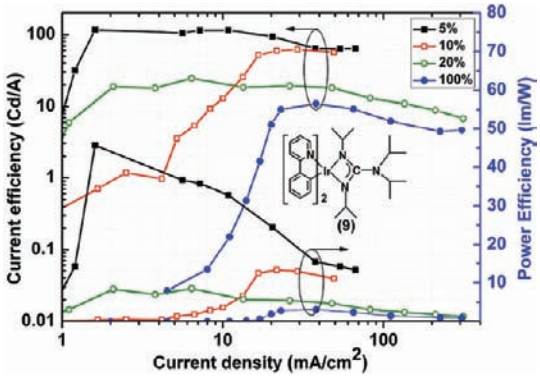

Figure 11. Current and power efficiencies of devices with different doping concentrations of complex **9**.

significant doping concentration dependence of the EL properties was observed. The device with 5% doping concentration showed the highest current efficiency (η_C = 116.43 cd/A) and power efficiency (η_P = 45.67 lm/W) at the current density of 1.6 mA/cm^2 and the maximum brightness (42 638 cd/m^2) at 15 V with λ_{max} = 560 nm. These values are among the best ever reported for yellow-emitting iridium complexes.[2c,22]

3. CONCLUSION

By the use of various guanidinate moieties as ancillary ligands, a novel family of structurally well-defined, phosphorescent heteroleptic cyclometalated iridium(III) complexes **1**−**11** have been prepared in high yields. These complexes show high phosphorescent quantum yields and short phosphorescent lifetimes at room temperature. The EL spectra of these complexes slightly shift from the corresponding PL spectra in the solid state and are independent of the applied voltage. Many of these complexes exhibit excellent EL properties such as high current efficiency, high power efficiency, and low turn-on voltage, and, more remarkably, their EL efficiencies are insensitive to the doping concentration in a wide range of current density. These properties make them highly desirable emitters for the efficient fabrication of high-performance EL devices. The excellent EL properties of the present complexes are obviously due to the sterically demanding and electron-donating properties of the ancillary guanidinate ligands, which could effectively protect the metal center and prevent significant T−T annihilation and nonemissive pathways caused by intermolecular excited-state interactions, as well as promotion of hole injection and hole transportation. Significant influences of the substituents in the guanidinate ligands on the fine structures and EL properties of the resulting complexes are also observed in many cases, which would therefore allow further improvement of the EL properties of such phosphorescent materials by modification of the ancillary ligands through substituent replacement. Further studies along this direction are in progress.

4. EXPERIMENTAL SECTION

4.1. Materials and Methods. All reactions were carried out under a dry and oxygen-free argon atmosphere by using Schlenk techniques or under a nitrogen atmosphere in an MBraun Lab master 130 glovebox. The nitrogen was purified by being passed through a dry clean column (4A molecular sieves, Nikka Seiko Co.) and a gas clean GC-XR column (Nikka Seiko Co.). The nitrogen in the glovebox was constantly circulating through a copper/molecular sieves catalyst unit. The oxygen and moisture concentrations in the glovebox atmosphere were monitored by an O_2/H_2O Combi-Analyzer to ensure both were always below 0.1 ppm. Materials obtained from a commercial supplier were used without further purification unless otherwise mentioned. THF, toluene, and diethyl ether (dehydrated, stabilizer-free) were obtained from Kanto Kagaku Co. and purified by use of a MBraun SPS-800 solvent purification system. Samples for NMR spectroscopic measurements were prepared in the glovebox by use of J. Young valve NMR tubes. NMR (^{1}H and ^{13}C) spectra were recorded on a JNM-AL 300 spectrometer. Elemental analyses (C, H, and N) were performed on a MICRO CORDER JM10 apparatus (J-SCIENCE LAB. Co.). The oxidation potential of iridium(III) complexes in acetonitrile was measured at a scan rate of 100 mV/s on a cyclic voltammeter (HSV-100-Hokuto Denko Corp.) with an electrochemical workstation, using platinum as the working electrode, platinum wire as the auxiliary electrode, and $Ag/AgNO_3$ as the reference electrode under a nitrogen atmosphere. Each measurement was calibrated with an internal standard, ferrocene/ferrocenium (Fc) redox system. The HOMO energy values were calculated based on the value of −4.8 eV for Fc with respect to zero vacuum level. Cyclometalated iridium(III) μ-chloride bridged dimer complex $[\{(ppy)_2Ir(\mu\text{-}Cl)\}_2]$ was synthesized according to the literature procedure.[23]

4.2. Synthesis of Ir(ppy)$_2$-*N,N′*-diisopropylguanidinate Complex [(ppy)$_2$Ir{(N^{i}Pr)$_2$C(NR^{1}R^2)}]. *[(ppy)$_2$Ir{(N^{i}Pr)$_2$C(NPh$_2$)}]* ***(1)***. In a 100 mL Schlenk flask, a hexane solution of *n*-BuLi (2.77 M, 0.14 mL, 0.4 mmol) was added to a solution of diphenylamine (67 mg, 0.4 mmol) in THF (5 mL) under argon at room temperature. The reaction mixture was stirred at room temperature for 2 h, and then *N,N′*-diisopropylcarbodiimide (50 mg, 0.4 mmol) was added dropwise to the reaction mixture. After 2 h of stirring, the reaction mixture was added dropwise to the iridium complex $[(ppy)_2Ir(\mu\text{-}Cl)]_2$ (0.2 mmol, 220 mg) in THF (15 mL). After being stirred at 80 °C for 16 h, the reaction mixture was cooled to room temperature, and the solvent was evaporated under vacuum. In order to remove THF completely, the residue was dissolved in toluene and was evaporated under reduced pressure. The product was dissolved again in toluene and was filtered to remove lithium chloride. The crude product was washed with Et_2O to give 255 mg of pure complex **1** (80% yield).

Single crystals of **1** suitable for X-ray analysis were grown in a CH_2Cl_2/acetone solution at room temperature. ^{1}H NMR (300 MHz, $CDCl_3$, rt): δ 9.20 (d, J = 5.5 Hz, 2 H, aryl), 7.89 (d, J = 8.1 Hz, 2 H, aryl), 7.79 (t, J = 7.5 Hz, 2 H, aryl), 7.56 (d, J = 7.3 Hz, 2 H, aryl), 7.24−7.29 (m, 6 H, aryl), 7.18 (d, J = 7.6 Hz, 4 H, aryl), 7.03 (t, J = 7.3 Hz, 2 H, aryl), 6.79 (t, J = 7.5 Hz, 2 H, aryl), 6.67 (t, J = 7.5 Hz, 2 H, aryl), 6.31 (d, J = 7.6 Hz, 2 H, aryl), 3.54−3.62 (m, 2 H, C*H*(CH$_3$)$_2$), 0.42 (d, J = 5.9 Hz, 6 H, CH (C*H*$_3$)$_2$), 0.11 (d, J = 6.2 Hz, 6 H, CH(C*H*$_3$)$_2$). ^{13}C NMR (75 MHz, $CDCl_3$, rt): δ 169.5, 160.7, 155.0, 152.3, 145.4, 144.4, 143.7, 135.5, 131.7, 128.8, 123.6, 122.2, 121.0, 120.7, 119.4, 117.9, 47.2, 24.5, 23.7. Anal. Calcd for $[C_{41}H_{40}IrN_5]$: C, 61.94; H, 5.07; N, 8.81. Found: C, 61.63; H, 5.07; N, 8.89.

[(ppy)$_2$Ir{(N^{i}Pr)$_2$CN(C$_6$H$_4$^{t}Bu-4)$_2$}] ***(2)***. According to the above-mentioned typical procedure, complex **2** (280 mg, 77% yield) was prepared from bis(4-*tert*-butylphenyl)amine (112 mg, 0.4 mmol), *n*-BuLi (0.14 mL, 0.4 mmol), *N,N′*-diisopropylcarbodiimide (50 mg, 0.4 mmol), and $[(ppy)_2Ir(\mu\text{-}Cl)]_2$ (220 mg, 0.2 mmol) in THF (15 mL). Single crystals of **2** suitable for X-ray analysis were grown in a toluene solution at room temperature in a glovebox. ^{1}H NMR (300 MHz, C_4D_8O, rt): δ 9.26 (d, J = 5.5 Hz, 2 H, aryl), 8.04 (d, J = 7.7 Hz, 2 H, aryl), 7.87 (t, J = 7.5 Hz, 2 H, aryl), 7.59 (d, J = 7.7 Hz, 2 H, aryl), 7.30−7.37 (m, 6 H, aryl), 7.08−7.14 (m, 4 H, aryl), 6.69 (t, J = 7.3 Hz, 2 H, aryl), 6.54 (t, J = 7.2 Hz, 2 H, aryl), 6.28 (d, J = 7.3 Hz, 2 H, aryl), 3.35−3.42 (m, 2 H, C*H*(CH$_3$)$_2$), 1.34 (s, 18 H, C(C*H*$_3$)$_3$), 0.41 (d, J = 6.2 Hz, 6 H, CH(C*H*$_3$)$_2$), 0.12 (d, J = 6.2 Hz, 6 H, CH(C*H*$_3$)$_2$). ^{13}C NMR (75 MHz, C_4D_8O, rt): δ 169.3, 161.4, 154.9, 152.3, 144.8, 144.6, 143.2, 135.8, 131.5, 128.4, 125.5, 123.5, 120.8, 120.6, 119.2, 118.0, 47.2, 33.9, 30.9, 24.2, 23.2. Anal. Calcd for $[C_{49}H_{56}IrN_5]$: C, 64.87; H, 6.22; N, 7.72. Found: C, 64.57; H, 6.31; N, 8.10.

[(ppy)$_2$Ir{(N^{i}Pr)$_2$C(carbazolyl)}] ***(3)***. According to the above-mentioned typical procedure, complex **3** (238 mg, 75% yield) was prepared from carbazole (67 mg, 0.4 mmol), *n*-BuLi (0.14 mL, 0.4

dx.doi.org/10.1021/ic201217a | *Inorg. Chem.* 2012, 51, 822−835

mmol), *N,N′*-diisopropylcarbodiimide (50 mg, 0.4 mmol), and $[(ppy)_2Ir(\mu\text{-}Cl)]_2$ (220 mg, 0.2 mmol) in THF (15 mL). Single crystals of **3** suitable for X-ray analysis were grown in a CH_2Cl_2/acetone solution at room temperature. ^{1}H NMR (300 MHz, $CDCl_3$, rt): δ 9.59 (d, J = 5.5 Hz, 2 H, aryl), 8.09 (d, J = 7.7 Hz, 2 H, aryl), 7.94 (d, J = 8.1 Hz, 2 H, aryl), 7.84 (t, J = 7.5 Hz, 2 H, aryl), 7.62 (d, J = 6.2 Hz, 4 H, aryl), 7.38−7.50 (m, 6 H, aryl), 6.84 (t, J = 7.3 Hz, 2 H, aryl), 6.73 (t, J = 7.3 Hz, 2 H, aryl), 6.42 (d, J = 7.7 Hz, 2 H, aryl), 3.02−3.06 (m, 2 H, $CH(CH_3)_2$), 0.64 (d, J = 6.2 Hz, 6 H, $CH(CH_3)_2$), −0.06 (d, J = 6.2 Hz, 6 H, $CH(CH_3)_2$). ^{13}C NMR (75 MHz, $CDCl_3$, rt): δ 169.7, 165.0, 159.8, 165.0, 153.6, 151.4, 144.1, 135.9, 131.9, 129.0, 126.1, 121.3, 120.3, 119.8, 119.8, 118.1, 116.1, 109.8, 47.4, 24.9, 24.0. Anal. Calcd for $[C_{41}H_{38}IrN_5]$: C, 62.10; H, 4.83; N, 8.83. Found: C, 62.35; H, 4.98; N, 8.76.

[(ppy)$_2$Ir{(N^{i}Pr)$_2$C(3,6-bis(tert-butyl)carbazolyl)}] ***(4)***. According to the above-mentioned typical procedure, complex **4** (254 mg, 70% yield) was prepared from (3,6-bis-*tert*-butyl)carbazole (112 mg, 0.4 mmol), *n*-BuLi (0.14 mL, 0.4 mmol), *N,N′*-diisopropylcarbodiimide (50 mg, 0.4 mmol), and $[(ppy)_2Ir(\mu\text{-}Cl)]_2$ (220 mg, 0.2 mmol) in THF (15 mL). Single crystals of **4** suitable for X-ray analysis were grown in a toluene solution at room temperature in a glovebox. ^{1}H NMR (300 MHz, C_4D_8O, rt): δ 9.63 (d, J = 4.8 Hz, 2 H, aryl), 8.14 (s, 2 H, aryl), 8.06 (d, J = 7.7 Hz, 2 H, aryl) 7.91 (d, J = 7.2 Hz, 2 H, aryl), 7.54−7.65 (m, 8 H, aryl), 6.73 (t, J = 7.0 Hz, 2 H, aryl), 6.60 (t, J = 7.0 Hz, 2 H, aryl), 6.37 (d, J = 7.2 Hz, 2 H, aryl), 3.11 (m, 2 H, $CH(CH_3)_2$), 1.44 (s, 18 H, $C(CH_3)_3$), 0.64 (d, J = 5.8 Hz, 6 H, $CH(CH_3)_2$), −0.06 (d, J = 5.0 Hz, 6 H, $CH(CH_3)_2$). ^{13}C NMR (75 MHz, C_4D_8O, rt): δ 169.7, 154.4, 153.8, 151.5, 144.4, 142.4, 138.4, 136.2, 131.7, 128.5, 123.7, 123.6, 122.8, 121.5, 119.4, 118.2, 116.3, 109.2, 47.4, 34.4, 31.4, 24.0, 23.5. Anal. Calcd for $[C_{49}H_{54}IrN_5]$: C, 65.02; H, 6.01; N, 7.74. Found: C, 65.04; H, 6.23; N, 8.06.

[(ppy)$_2$Ir{(N^{i}Pr)$_2$CN(C$_6$H$_4$)$_2$S}] ***(5)***. According to the above-mentioned typical procedure, complex **5** (232 mg, 70% yield) was prepared from phenothiazine (80 mg, 0.4 mmol), *n*-BuLi (0.14 mL, 0.4 mmol), *N,N′*-diisopropylcarbodiimide (50 mg, 0.4 mmol), and $[(ppy)_2Ir(\mu\text{-}Cl)]_2$ (220 mg, 0.2 mmol in THF (15 mL). Single crystals of **5** suitable for X-ray analysis were grown in a CH_2Cl_2/acetone solution at room temperature. ^{1}H NMR (300 MHz, C_4D_8O, rt): δ 9.36 (d, J = 5.7 Hz, 2 H, aryl), 8.04 (d, J = 7.6 Hz, 2 H, aryl), 7.89 (t, J = 7.6 Hz, 2 H, aryl), 7.64 (d, J = 7.6 Hz, 2 H, aryl), 7.37 (t, J = 6.4 Hz, 2 H, aryl), 7.11 (d, J = 7.6 Hz, 2 H, aryl), 6.96 (t, J = 7.4 Hz, 2 H, aryl), 6.69−6.84 (m, 6 H, aryl), 6.60 (t, J = 7.6 Hz, 2 H, aryl), 6.35 (d, J = 7.6 Hz, 2 H, aryl), 3.74−3.83 (m, 2 H, $CH(CH_3)_2$), 0.83 (d, J = 6.2 Hz, 6 H, $CH(CH_3)_2$), 0.12 (d, J = 6.2 Hz, 6 H, $CH(CH_3)_2$). ^{13}C NMR (75 MHz, C_4D_8O, rt): δ 169.8, 163.4, 161.1, 153.5, 152.3, 144.6, 140.2, 136.4, 131.6, 128.5, 126.3, 123.7, 122.7, 121.0, 119.6, 118.8, 118.2, 116.1, 47.3, 23.8, 23.5. Anal. Calcd for $[C_{41}H_{38}IrN_5S]$: C, 59.69.; H, 4.64; N, 8.49. Found: C, 59.68; H, 4.88; N, 8.55.

[(ppy)$_2$Ir{(N^{i}Pr)$_2$CN(C$_6$H$_4$)$_2$O}] ***(6)***. According to the above-mentioned typical procedure, complex **6** (228 mg, 70% yield) was prepared from phenoxazine (73 mg, 0.4 mmol), *n*-BuLi (0.14 mL, 0.4 mmol), *N,N′*-diisopropylcarbodiimide (50 mg, 0.4 mmol), and $[(ppy)_2Ir(\mu\text{-}Cl)]_2$ (220 mg, 0.2 mmol) in THF (15 mL). Single crystals of **6** suitable for X-ray analysis were grown in a CH_2Cl_2/acetone solution at room temperature. ^{1}H NMR (300 MHz, C_4D_8O, rt): δ 9.40 (d, J = 5.0 Hz, 2 H, aryl), 8.04 (d, J = 8.0 Hz, 2 H, aryl) 7.90 (t, J = 7.0 Hz, 2 H, aryl), 7.64 (d, J = 7.0 Hz, 2 H, aryl), 7.40 (t, J = 9.0 Hz, 2 H, aryl), 6.93 (d, J = 8.0 Hz, 2 H, aryl), 6.58−6.74 (m, 10 H, aryl), 6.34 (d, J = 8.0 Hz, 2 H, aryl), 3.73−3.77 (m, 2 H, $CH(CH_3)_2$), 0.80 (d, J = 5.0 Hz, 6 H, $CH(CH_3)_2$), 0.10 (d, J = 5.0 Hz, 6 H, $CH(CH_3)_2$). ^{13}C NMR (75 MHz, C_4D_8O, rt): δ 170.0, 153.8, 153.3, 152.2, 144.4, 143.05, 136.4, 131.6, 131.1, 128.5, 123.7, 122.9, 121.8, 121.1, 119.6, 118.2, 115.6, 113.7, 47.3, 23.8. Anal. Calcd for $[C_{41}H_{38}IrN_5O]$: C, 60.87; H, 4.73; N, 8.66. Found: C, 60.56; H, 4.90; N, 8.91.

[(ppy)$_2$Ir{(N^{i}Pr)$_2$C(indolyl)}] ***(7)***. According to the above-mentioned typical procedure, complex **7** (210 mg, 71% yield) was prepared from indole (47 mg, 0.4 mmol), *n*-BuLi (0.14 mL, 0.4 mmol), *N,N′*-diisopropylcarbodiimide (50 mg, 0.4 mmol), and $[(ppy)_2Ir(\mu\text{-}Cl)]_2$ (220 mg, 0.2 mmol) in THF (15 mL). Single crystals of **7** suitable for X-ray analysis were grown in a CH_2Cl_2/acetone solution at room temperature. ^{1}H NMR (300 MHz, C_4D_8O, rt): δ 9.51 (d, J = 6.0 Hz, 1 H, aryl), 9.28 (d, J = 6.0 Hz, 1H, aryl), 7.98 (d, J = 8.0 Hz, 2 H, aryl), 7.83 (d, J = 7.0 Hz, 1 H, aryl), 7.78 (d, J = 8.0 Hz, 1 H, aryl), 7.57−7.48 (m, 4 H, aryl), 7.42 (t, J = 6.5 Hz, 1 H, aryl), 7.32 (t, J = 7.0 Hz, 1 H, aryl), 7.20−7.13 (m, 2 H, aryl), 7.03 (t, J = 7.0 Hz, 1 H, aryl), 6.67 (t, J = 7.0 Hz, 2 H, aryl), 6.48−6.53 (m, 3 H, aryl), 6.29 (t, J = 8.5 Hz, 2 H, aryl), 3.17−3.10 (m, 2 H, $CH(CH_3)_2$), 0.06 (d, J = 5.0 Hz, 6 H, $CH(CH_3)_2$), −0.10 (d, J = 6.0 Hz, 6 H, $CH(CH_3)_2$). ^{13}C NMR (75 MHz, C_4D_8O, rt): δ 169.6, 162.9, 155.5, 153.5, 151.3, 151.2, 150.6, 144.4, 136.0, 135.8, 135.6, 131.9, 128.5, 128.1, 126.7, 123.6, 123.3, 122.4, 121.6, 121.5, 121.1, 120.7, 120.0, 119.5, 119.4, 119.1, 118.2, 117.6, 110.2, 102.4, 47.3, 23.4. Anal. Calcd for $[C_{37}H_{36}IrN_5]$: C, 59.82; H, 4.88; N, 9.43. Found: C, 59.63; H, 4.98; N, 9.81.

[(ppy)$_2$Ir{(N^{i}Pr)$_2$C(NEt$_2$)}] ***(8)***. According to the above-mentioned typical procedure, complex **8** (168 mg, 60% yield) was prepared from diethylamine (29 mg, 0.4 mmol), *n*-BuLi (0.14 mL, 0.4 mmol), *N,N′*-diisopropylcarbodiimide (50 mg, 0.4 mmol), and $[(ppy)_2Ir(\mu\text{-}Cl)]_2$ (220 mg, 0.2 mmol) in THF (15 mL). Single crystals of **8** suitable for X-ray analysis were grown in a toluene/ether solution at room temperature. ^{1}H NMR (300 MHz, C_4D_8O, rt): δ 9.25 (d, J = 5.8 Hz, 2 H, aryl), 7.95 (d, J = 8.1 Hz, 2 H, aryl), 7.75 (t, J = 7.7 Hz, 2 H, aryl), 7.56 (d, J = 7.7 Hz, 2 H, aryl), 7.22 (t, J = 6.6 Hz, 2 H, aryl), 6.66 (t, J = 7.3 Hz, 2 H, aryl), 6.49 (t, J = 7.3 Hz, 2 H, aryl), 6.23 (d, J = 7.7 Hz, 2 H, aryl), 3.67−3.75 (m, 2 H, $CH(CH_3)_2$), 3.23−3.02 (m, 4 H, CH_2CH_3), 1.11 (t, J = 7.0 Hz, 6 H, CH_2CH_3), 0.77 (d, J = 6.2 Hz, 6 H, $CH(CH_3)_2$), −0.01 (d, J = 6.2 Hz, 6 H, $CH(CH_3)_2$). ^{13}C NMR (75 MHz, C_4D_8O, rt): δ 169.9, 168.8, 156.7, 151.0, 144.4, 135.1, 131.5, 128.3, 120.85, 118.8, 117.8, 47.4, 44.4, 23.8, 23.7, 13.8. Anal. Calcd for $[C_{33}H_{40}IrN_5]$: C, 56.71; H, 5.77; N, 10.02. Found: C, 56.37; H, 5.79; N, 10.34.

[(ppy)$_2$Ir{(N^{i}Pr)$_2$C(N^{i}Pr$_2$)}] ***(9)***. According to the above-mentioned typical procedure, complex **9** (204 mg, 70% yield) was prepared from diisopropylamine (41 mg, 0.4 mmol), *n*-BuLi (0.14 mL, 0.4 mmol), *N,N′*-diisopropylcarbodiimide (50 mg, 0.4 mmol), and $[(ppy)_2Ir(\mu\text{-}Cl)]_2$ (220 mg, 0.2 mmol) in THF (15 mL). Single crystals of **9** suitable for X-ray analysis were grown in a CH_2Cl_2/acetone solution at room temperature. ^{1}H NMR (300 MHz, C_6D_6, rt): δ 9.35 (d, J = 5.5 Hz, 2 H, aryl), 7.52 (d, J = 7.3 Hz, 2 H, aryl), 7.41 (d, J = 8.1 Hz, 2 H, aryl), 7.02 (t, J = 7.1 Hz, 2 H, aryl), 6.73−6.87 (m, 6 H, aryl), 6.67 (t, J = 6.4 Hz, 2 H, aryl), 3.88−3.93 (m, 2 H, $CH(CH_3)_2$), 3.44−3.48 (m, 2 H, $CH(CH_3)_2$), 1.08−1.21 (m, 12 H, $CH(CH_3)_2$), 1.10 (d, J = 6.2 Hz, 6 H, $CH(CH_3)_2$), 0.25 (d, J = 6.2 Hz, 6 H, $CH(CH_3)_2$). ^{13}C NMR (75 MHz, C_6D_6, rt): δ 170.4, 168.2, 157.5, 151.8, 144.6, 134.9, 132.2, 129.6, 124.2, 120.4, 119.9, 117.9, 49.2, 47.7, 24.8, 24.4, 24.2, 22.9. Anal. Calcd for $[C_{35}H_{44}IrN_5]$: C, 57.83; H, 6.10; N, 9.63. Found: C, 57.58; H, 6.04; N, 9.61.

[(ppy)$_2$Ir{(N^{i}Pr)$_2$C(N^{i}Bu$_2$)}] ***(10)***. According to the above-mentioned typical procedure, complex **10** (225 mg, 75% yield) was prepared from diisobutylamine (52 mg, 0.4 mmol), *n*-BuLi (0.14 mL, 0.4 mmol), *N,N′*-diisopropylcarbodiimide (50 mg, 0.4 mmol), and $[(ppy)_2Ir(\mu\text{-}Cl)]_2$ (220 mg, 0.2 mmol) in THF (15 mL). Single crystals of **10** suitable for X-ray analysis were grown in a toluene solution at room temperature in a glovebox. ^{1}H NMR (300 MHz, C_4D_8O, rt): δ 9.20 (d, J = 5.5 Hz, 2 H, aryl), 7.87 (d, J = 8.1 Hz, 2 H, aryl), 7.69 (t, J = 7.7 Hz, 2 H, aryl), 7.49 (d, J = 7.7 Hz, 2 H, aryl), 7.15 (t, J = 6.2 Hz, 2 H, aryl), 6.59 (t, J = 7.1 Hz, 2 H, aryl), 6.46 (t, J = 7.0 Hz, 2 H, aryl), 6.17 (d, J = 7.3 Hz, 2 H, aryl), 3.71−3.79 (m, 2 H, $CH(CH_3)_2$), 2.80−2.94 (m, 4 H, CH_2CH), 1.80−1.89 (m, 2 H, CH_2CH), 0.89 (d, J = 6.2 Hz, 12 H, $CH(CH_3)_2$), 0.82 (d, J = 6.2 Hz, 6 H, $CH(CH_3)_2$), −0.11 (d, J = 6.2 Hz, 6 H, $CH(CH_3)_2$). ^{13}C NMR (75 MHz, C_4D_8O, rt): δ 170.0, 169.0, 161.1, 159.1, 151.1, 144.5, 135.1, 131.5, 128.34, 123.4, 120.6, 118.8, 117.8, 59.5, 47.7, 27.5, 23.2, 20.4, 20.2. Anal. Calcd for $[C_{37}H_{48}IrN_5]$: C, 58.86; H, 6.41; N, 9.28. Found: C, 58.80; H, 6.45; N, 9.43.

[(ppy)$_2$Ir{(N^{i}Pr)$_2$CN(SiMe$_3$)$_2$}] ***(11)***. According to the above-mentioned typical procedure, complex **11** (220 mg, 70% yield) was prepared from lithium bis(trimethylsilyl)amide (67 mg, 0.4 mmol), *N,N′*-diisopropylcarbodiimide (50 mg, 0.4 mmol), and $[(ppy)_2Ir(\mu\text{-}Cl)]_2$ (220 mg, 0.2 mmol) in THF (15 mL). Single crystals of **11** suitable for X-ray analysis were grown in a CH_2Cl_2/acetone solution at

dx.doi.org/10.1021/ic201217a | *Inorg. Chem.* 2012, 51, 822−835

Table 5. Summary of the Crystallographic Data of 1−6

	1	2·toluene	3	4·2(toluene)	5	6
empirical formula	$C_{41}H_{40}IrN_5$	$C_{56}H_{65}IrN_5$	$C_{41}H_{38}IrN_5$	$C_{63}H_{70}IrN_5$	$C_{41}H_{38}IrN_5S$	$C_{41}H_{38}IrN_5O$
fw	794.98	999.32	792.96	1089.44	825.02	808.96
temp (K)	173	173	173	173	173(2)	173(2)
cryst syst	monoclinic	monoclinic	triclinic	triclinic	monoclinic	monoclinic
space group	$P2(1)/n$	$P2(1)/n$	$P\bar{1}$	$P\bar{1}$	$P2(1)/n$	$P2(1)/n$
a (Å)	9.3240(14)	14.5028(18)	12.064(2)	11.112(4)	9.4249(11)	9.482(4)
b (Å)	38.685(6)	15.1337(18)	12.613(2)	15.742(5)	38.875(5)	37.636(17)
c (Å)	10.3325(15)	22.409 (3)	13.605(2)	16.584(5)	10.2628(12)	10.311(5)
α (deg)	90	90	101.863(2)	112.386(4)	90	90
β (deg)	113.095(2)	105.361(2)	103.870(2)	96.055(4)	113.795(1)	112.892(7)
γ (deg)	90	90	117.480(2)	97.321(4)	90	90
V (Å^3)	3428.2(9)	4742(10)	1658.6(5)	2622.8(14)	3440.6(7)	3390(3)
Z	4	4	2	2	4	4
density (calcd) (g/cm^3	1.54	1.4	1.588	1.379	1.593	1.585
abs coeff (mm^{-1})	3.913	2.858	4.063	2.59	3.979	3.98
$F(000)$	1592	2048	792	1120	1648	1616
θ range (deg)	2.11−25.06	1.51−25.04	1.66−25.09	1.42−25.04	2.10−25.06	2.16−25.11
reflns collected	17 805	24 847	8572	13 733	18 225	18 517
indep reflns (R_{int})	6029(0.0603)	8367(0.0410)	5605(0.0301)	8817(0.0565)	6052(0.0510)	6005(0.0851)
data/restraints/param	6029/0/428	8367/0/559	5605/0/409	8817/0/616	6052/0/432	6005/0/43
GOF on F^2	1.096	0.89	1.062	0.984	1.197	0.967
final R index [$I > 2\sigma(I)$]	0.0488	0.0288	0.0505	0.0597	0.0475	0.0534
R_w	0.107	0.0492	0.1393	0.1356	0.1039	0.1056

Table 6. Summary of the Crystallographic Data of 7−11

	7·0.5(acetone)	8	9	10	11
empirical formula	$C_{77}H_{78}Ir_2N_{10}O$	$C_{33}H_{40}IrN_5$	$C_{35}H_{44}IrN_5$	$C_{37}H_{48}IrN_5$	$C_{35}H_{48}IrN_5Si_2$
fw	1543.89	698.90	726.95	755.00	787.16
temp (K)	173(2)	173 (2)	173 (2)	173 (2)	173 (2)
cryst syst	monoclinic	monoclinic	triclinic	monoclinic	monoclinic
space group	$C2/c$	$C2/c$	$P\bar{1}$	$C2/c$	$P2(1)/n$
a (Å)	22.451(6)	16.330 (6)	9.7802 (12)	30.633 (4)	11.968 (4)
b (Å)	12.203(3)	11.948 (4)	11.7240 (15)	22.071 (3)	32.511 (11)
c (Å)	26.487(6)	30.927 (12)	15.3546 (19)	16.436 (2)	18.857 (6)
α (deg)	90	90	92.770 (2)	90	90
β (deg)	114.07(6)	94.737 (5)	93.282 (2)	112.643 (2)	108.205 (5)
γ (deg)	90	90	114.310 (2)	90	90
V (Å^3)	6626(3)	6014 (4)	1596.9 (3)	10256 (2)	6970(4)
Z	4	8	2	12	8
density (calcd)(g/cm^3)	1.548	1.544	1.512	1.467	1.5
abs coeff (mm^{-1})	4.067	4.47	4.212	3.938	3.931
$F(000)$	3088	2800	732	4584	3184
θ range (deg)	1.68−25.22	2.11−25.11	1.33−25.03	1.56−25.04	1.69−25.09
reflns collected	16 509	14 726	7923	26 403	36 223
indep reflns (R_{int})	5947(0.0662)	5264 (0.1006)	5317 (0.0366)	9029 (0.0444)	12330 (0.1132)
data/restraints/param	5947/0/412	5264/0/332	5317/0/360	9029/0/595	12 330/0/765
GOF on F^2	1.071	1.085	1.144	0.94	1.041
final R index [$I > 2\sigma(I)$]	0.0552	0.0741	0.0445	0.029	0.0869
R_w	0.966	0.1579	0.1290	0.0557	0.1819

room temperature. ^{1}H NMR (300 MHz, C_6D_6, rt): δ 9.45 (d, J = 5.3 Hz, 2 H, aryl), 7.50 (d, J = 7.7 Hz, 2 H, aryl), 7.43 (d, J = 7.7 Hz, 2 H, aryl), 7.09 (t, J = 8.0 Hz, 2 H, aryl), 6.71−6.85 (m, 6 H, aryl), 6.64 (d, J = 7.2 Hz, 2 H, aryl), 3.88−3.93 (m, 2 H, $CH(CH_3)_2$), 1.09 (d, J = 6.3 Hz, 6 H, $CH(CH_3)_2$), 0.34 (d, J = 6.3 Hz, 6 H, $CH(CH_3)_2$), 0.28 (s, 18 H, $SiMe_3$). ^{13}C NMR (75 MHz, C_4D_8O, rt): δ 170.0, 162.9, 156.0, 153.8, 144.9, 135.1, 131.7, 129.4, 124.2, 120.6, 120.0, 117.7, 47.2, 25.4, 25.1, 3.4. Anal. Calcd for [$C_{35}H_{48}IrN_5Si_2$]: C, 53.40; H, 6.15; N, 8.90. Found: C, 53.73; H, 6.20; N, 9.04.

4.3. Optical Measurements. The absorption and PL spectra of iridium(III) complexes in degassed dichloromethane were measured on a Shimadzu UV-2550 UV−vis spectrometer and on a Shimadzu RF-5301PC fluorescence spectrometer with a xenon arc lamp excitation source, respectively. Solutions for the measurements of PL quantum yields (Φ) and lifetimes were freshly prepared by dissolving iridium complexes into degassed THF at ~10^{-5} M concentration to make absorbance below 0.1. The solution PL quantum yields (Φ) were measured three times relative to quinine sulfate in 1 N H_2SO_4 assuming a quantum yield of 0.546 when excited at 350 nm and corrected for the solvent refractive index. Emission lifetime measurements were carried out three times by using a streak-camera-based system (Hamamatsu, C4780) combined with a femtosecond

dx.doi.org/10.1021/ic201217a | Inorg. Chem. 2012, 51, 822−835

Ti:sapphire laser system (Spectra-Physics, Spitfire). The excitation and detection wavelengths were 397 and 450−700 nm, respectively. The time resolution was 30−40 ns.

4.4. OLED Fabrication and Characterization. Organic layers were fabricated by high-vacuum (10^{-4} Pa) thermal evaporation onto a glass substrate precoated with an ITO layer (Sigma Aldrich) with a sheet resistance of 12−25 Ω/□. Prior to use, the ITO (anode) surface was ultrasonicated in a detergent solution followed by a deionized water rinse, dipped in acetone and 2-propanol, and then degreased in 2-propanol vapor. After degreasing, the substrate was kept in an oven for drying at 80 °C for 2 h. Prior to organic film deposition, the ITO surface was treated with an UV-ozone chamber for 10 min before it was loaded into an evaporator. A 30-nm-thick layer of NPB acts as an HTL. A light-emitting layer (25 nm) consisting of 5−20 wt % iridium complexes doped into host CBP as well as pure iridium complexes was used. A 6-nm-thick BCP as an HBL and Alq_3 (20 nm) as an ETL were deposited on the emitting layer. An LiF layer (1 nm) was deposited at a rate of 0.2 Å/s serving as an electron injection layer. Finally, an aluminum (100 nm) electrode (cathode) was deposited at a rate of 10 Å/s. All of these complexes were vacuum-deposited without any decomposition and showed very good film forming. The deposition rate for all organic layers was 1.0 Å/s. The thickness of the deposited layers was measured in situ with a quartz crystal monitor. The size of each pixel was 5 × 5 mm^2. The EL spectra have been measured on a high-resolution spectrometer (Stellar net Blue-wave UV−vis−near-IR). The *I*−*V*−*L* characteristics were measured with a luminance meter (Chroma-Meter CS-200 Konika Minolta, Japan) and a Keithley-2400 programmable voltage−current digital source meter. All the measurements were carried out at room temperature under ambient conditions.

4.5. X-ray Crystallographic Studies. A crystal was sealed in a thin-walled glass capillary under a microscope in the glovebox. Data collections were performed at −100 °C on a Bruker SMART APEX diffractometer with a CCD area detector using graphite-monochromated Mo Kα radiation (λ = 0.710 69 Å). Determination of the crystal class and unit cell parameters was carried out by the *SMART* program package.[24] The raw frame data were processed using *SAINT*[25] and *SADABS*[26] to yield the reflection data file. The structures were solved by using the *SHELXTL* program.[27] Refinements were performed on F^2 anisotropically for all of the non-hydrogen atoms by the full-matrix least-squares method. The analytical scattering factors for neutral atoms were used throughout the analysis. The hydrogen atoms were placed at the calculated positions and were included in the structure calculation without further refinement of the parameters. The residual electron densities were of no chemical significance. Crystal data and processing parameters are summarized in Tables 5 and 6.

Crystallographic data (excluding structure factors) have been deposited with the Cambridge Crystallographic Data Centre as supplementary publications CCDC 808964 (**1**), 808972 (**2**), 808970 (**3**), 808971 (**4**), 808969 (**5**), 808963 (**6**), 808973 (**7**), 808965 (**8**), 808967 (**9**), 808966 (**10**), and 808968 (**11**). Copies of these data can be obtained free of charge from the Cambridge Crystallographic Data Centre via www.ccdc.cam.ac.uk/data_request/cif.

4.6. DFT Calculations. The ground state was fully optimized by the DFT[28] method with Becke's three-parameter functional and the Lee−Yang−Parr functional[29] (B3LYP). In the calculations, "double-ζ"-quality and polarization basis sets were employed for the ligands [6-31G(d)] and iridium (LANL2DZ). A relativistic effective core potential on Ir[30] replaced the inner-core electrons, leaving the outer-core [$(5s)^2(5p)^6$] electrons and the $(5d)^6$ valence electrons of iridium(III). On the basis of the optimized ground state, the absorption property in dichloromethane (CH_2Cl_2) media was calculated by time-dependent DFT[31] associated with the polarized continuum model.[32] This kind of theoretical approach has been proven to be reliable for transition-metal complex systems.[33] All of the calculations were accomplished by using the *Gaussian 03* software package.[34]

■ ASSOCIATED CONTENT

Ⓢ Supporting Information

Crystallographic data in CIF format of all complexes (**1**−**11**), phosphorescent lifetime, cyclic voltammgrams, and performance data for all OLEDs. This material is available free of charge via the Internet at http://pubs.acs.org.

■ AUTHOR INFORMATION

Corresponding Author

*E-mail: houz@riken.jp.

■ ACKNOWLEDGMENTS

This work was supported by a Grant-in-Aid for Scientific Research (S) (Grant 21225004 to Z.H.) and for Young Scientists (Grant 22750062 to M.N.) from Ministry of Education, Culture, Sports, Science and Technology (MEXT), Japan. We thank Prof. T. Tahara and Dr. K. Ishii for phosphorescent lifetime measurements and Ms. Karube for elemental analysis.

■ REFERENCES

(1) (a) Baldo, M. A.; Thompson, M. E.; Forrest, S. R. *Nature* **2000**, *403*, 750. (b) Friend, R. H.; Gymer, R. W.; Holmes, A. B.; Burroughes, J. H.; Marks, R. N.; Taliani, C.; Bradley, D. D. C.; Dos Santos, D. A.; Bredas, J. L.; Logdlund, M.; Salaneck, W. R. *Nature* **1999**, *397*, 121. (c) D'Andrade, B. W.; Forrest, S. R. *Adv. Mater.* **2004**, *16*, 1585. (d) Burn, P. L.; Lo, S. C.; Samuel, I. D. W. *Adv. Mater.* **2007**, *19*, 1675. (e) Kido, J.; Kimura, M.; Nagai, K. *Science* **1995**, *267*, 1332. (f) Duggal, R.; Shiang, J. J.; Heller, C. M.; Foust, D. F. *Appl. Phys. Lett.* **2002**, *80*, 3470. (g) Forrest, S. R. *Org. Electron.* **2003**, *4*, 45. (h) David, M. C.; Falcou, A.; Reckefuss, N.; Rojahn, M.; Wiederhirn, V.; Rudati, P.; Frohne, H.; Nuyken, O.; Becker, H.; Meerholz, K. *Nature* **2003**, *421*, 829. (i) Elisabeth, H.; Langeveld, B. M.; Ulrich, S. S. *Adv. Mater.* **2005**, *17*, 1109.

(2) (a) Baldo, M. A.; O'Brien, D. F.; You, Y.; Shoustikov, A.; Sibley, S.; Thompson, M. E.; Forrest, S. R. *Nature* **1998**, *395*, 151. (b) Sun, Y.; Noel, C. G.; Hiroshi, K.; Biwu, M.; Thompson, M. E.; Forrest, S. R. *Nature* **2006**, *440*, 908. (c) Lamansky, S.; Djurovich, P.; Murphy, D.; Razzaq, F. A.; Lee, H. E.; Adachi, C.; Burrows, P. E.; Forrest, S. R.; Thompson, M. E. *J. Am. Chem. Soc.* **2001**, *123*, 4304. (d) Lamansky, S.; Djurovich, P. I.; Razzaq, F. A.; Garon, S.; Murphy, D. L.; Thompson, M. E. *J. Appl. Phys.* **2002**, *92*, 1570. (e) Tamayo, A. B.; Alleyne, B. D.; Djurovich, P. I.; Lamansky, S.; Tsyba, I.; Ho, N. N.; Bau, R.; Thompson, M. E. *J. Am. Chem. Soc.* **2003**, *125*, 7377. (f) D'Andrade, B. W.; Holmes, R. J.; Forrest, S. R. *Adv. Mater.* **2004**, *16*, 624. (g) Li, J.; Djurovich, P. I.; Alleyne, B. D.; Yousufuddin, M.; Ho, N. N.; Thomas, J. C.; Peters, J. C.; Bau, R.; Thompson, M. E. *Inorg. Chem.* **2005**, *44*, 1713. (h) Sajoto, T.; Djurovich, P. I.; Tamayo, A.; Yousufuddin, M.; Bau, R.; Thompson, M. E.; Holmes, R. J.; Forrest, S. R. *Inorg. Chem.* **2005**, *44*, 7992. (i) Adachi, C.; Baldo, M. A.; Thompson, M. E.; Forrest, S. R. *J. Appl. Phys.* **2001**, *90*, 5048. (j) Baldo, M. A.; Lamansky, S.; Burrows, P. E.; Thompson, M. E.; Forrest, S. R. *Appl. Phys. Lett.* **1999**, *75*, 4. (k) Gufeng, H.; Pfeiffer, M.; Karl, L.; Hofmann, M.; Birnstock, J.; Robert, P.; Josef, S. *Appl. Phys. Lett.* **2004**, *85*, 3911. (l) Peng, H. J.; Zhu, X. L.; Sun, J. X.; Yu, X. M.; Wong, M.; Kwok, H. S. *Appl. Phys. Lett.* **2006**, *88*, 33509. (m) Sebastian, R.; Frank, L.; Gregor, S.; Nico, S.; Walzer, K.; Lussem, B.; Karl, L. *Nature* **2009**, *459*, 234. (n) Ulbricht, C.; Beyer, B.; Friebe, C.; Winter, A.; Schubert, U. S. *Adv. Mater.* **2009**, *21*, 4418. (o) Bolink, H. J.; Cappelli, L.; Coronado, E.; Grätzel, M.; Orti, E.; Costa, R. D.; Viruela, P. M.; Nazeeruddin, M. K. *J. Am. Chem. Soc.* **2006**, *128*, 14786. (p) Wenjuan, X.; Shujuan, L.; Huibin, S.; Xinyan, Z.; Qiang, Z.; Shi, S.; Shan, C.; Tingchun, M.; Lixia, Z.; Wei, H. *J. Mater. Chem.* **2011**, *21*, 7572. (q) Xu, W.-J.; Liu, S.-J.; Zhao, X.-Y.; Shi, S.; Shan, C.; Ma, T.-C.; Sun, H.-B.; Qiang, Z.; Wei, H. *Chem.—Eur. J.* **2010**, *16*, 7125. (r) Shi, H.-F.; Liu, S.-J.; Sun, H.-B.; Xu, W.-J.; An, Z.-F.; Jian, C.; Shi, S.; Lu, X.-M.; Qiang, Z.; Wei, H.

Chem.—Eur. J. **2010**, *16*, 12158. (s) Qiang, Z.; Chunhui, H.; Fuyou, L. *Chem. Soc. Rev.* **2011**, *40*, 2508. (t) Huazhou, W.; Tianshe, Y.; Qiang, Z.; Jing, Z.; Chunyan, L.; Fuyou, L. *Dalton Trans.* **2011**, *40*, 1969. (u) Qiang, Z.; Fuyou, L.; Chunhui, H. *Chem. Soc. Rev.* **2010**, *39*, 3007. (v) Chi, Y.; Chou, P.-T. *Chem. Soc. Rev.* **2010**, *39*, 638.

(3) (a) Lamansky, S.; Djurovich, P.; Murphy, D.; Abdel-Razzaq, F.; Kwong, R.; Tsyba, I.; Bortz, M.; Mui, B.; Bau, R.; Thompson, M. E. *Inorg. Chem.* **2001**, *40*, 1704. (b) You, Y.; Park, S. Y. *J. Am. Chem. Soc.* **2005**, *127*, 12438. (c) Ragni, R.; Plummer, E. A.; Brunner, K.; Hofstraat, J. W.; Babudri, F.; Farinola, G. M.; Naso, F.; De Cola, L. *J. Mater. Chem.* **2006**, *16*, 1161. (d) Kwon, T.-H.; Cho, H. S.; Kim, M. K.; Kim, J.-W.; Kim, J.-J.; Lee, K. H.; Park, S. J.; Shin, I.-S.; Kim, H.; Shin, D. M.; Chung, Y. K.; Hong, J.-I. *Organometallics* **2005**, *24*, 1578. (e) Zhao, Q.; Liu, S.; Shi, M.; Wang, C.; Yu, M.; Li, L.; Li, F.; Yi, T.; Huang, C. *Inorg. Chem.* **2006**, *45*, 6152. (f) Avilov, I.; Minoofar, P.; Cornil, J.; De Cola, L. *J. Am. Chem. Soc.* **2007**, *129*, 8247. (g) Stagni, S.; Colella, S.; Palazzi, A.; Valenti, G.; Zacchini, S.; Paolucci, F.; Marcaccio, M.; Albuquerque, R. Q.; De Cola, L. *Inorg. Chem.* **2008**, *47*, 10509. (h) Rai, V. K.; Nishiura, M.; Takimoto, M.; Hou, Z. *Chem. Commun.* **2011**, *47*, 5726.

(4) (a) Chang, C.-J.; Yang, C.-H.; Chen, K.; Chi, Y.; Shu, C.-F.; Ho, M.-L.; Yeh, Y.-S.; Chou, P.-T. *Dalton Trans.* **2007**, *19*, 1881. (b) Wang, Y.-M.; Teng, F.; Gan, L.-H.; Liu, H.-M.; Zhang, X.-H.; Fu, W.-F.; Wang, Y.-S.; Xu, X.-R. *J. Phys. Chem. C* **2008**, *112*, 4743. (c) Yeh, S.-J.; Wu, M.-F.; Chen, C.-T.; Song, Y.-H.; Chi, Y.; Ho, M.-H.; Hsu, S.-F.; Chen, C. H. *Adv. Mater.* **2005**, *17*, 285. (d) Li, J.; Djurovich, P. I.; Alleyne, B. D.; Tsyba, I.; Ho, N. N.; Bau, R.; Thompson, M. E. *Polyhedron* **2004**, *23*, 419. (e) Nazeeruddin, M. K.; Humphry-Baker, R.; Berner, D.; Rivier, S.; Zuppiroli, L.; Graetzel, M. *J. Am. Chem. Soc.* **2003**, *125*, 8790. (f) Coppo, P.; Plummer, E. A.; De Cola, L. *Chem. Commun.* **2004**, *15*, 1774. (g) Lee, T.-C.; Chang, C.-F.; Chiu, Y.-C.; Chi, Y.; Chan, T.-Y.; Cheng, Y.-M.; Lai, C.-H.; Chou, P.-T.; Lee, G.-H.; Chien, C.-H.; Shu, C.-F.; Leonhardt, J. *Chem.—Asian. J.* **2009**, *4*, 742. (h) Hanson, K.; Tamayo, A.; Diev, V. V.; Whited, M. T.; Djurovich, P. I.; Thompson, M. E. *Inorg. Chem.* **2010**, *49*, 6077. (i) You, Y.; Park, S. Y. *Dalton Trans.* **2009**, 1267. (j) Li, X.; Chen, Z.; Zhao, Q.; Shen, L.; Li, F.; Yi, T.; Cao, Y.; Huang, C. *Inorg. Chem.* **2007**, *46*, 5518. (k) Velusamy, M.; Thomas, K. R. J.; Chen, C.-H.; Lin, J. T.; Wen, Y. S.; Hsieh, W.-T.; Lai, C.-H.; Chou, P.-T. *Dalton Trans.* **2007**, 3025.

(5) (a) Baldo, M. A.; Adachi, C.; Forrest, S. R. *Phys. Rev. B* **2000**, *62*, 10967. (b) Sebastian, R.; Walzer, K.; Leo, K. *Phys. Rev. B* **2007**, *75*, 125328. (c) Starsoke, W.; Pfeiffer, M.; Leo, K.; Hoffmann, M. *Phys. Rev. Lett.* **2007**, *98*, 197402.

(6) (a) Liu, Y.; Ye, K.; Fan, Y.; Song, W.; Wang, Y.; Hou, Z. *Chem. Commun.* **2009**, 3699. (b) Peng, T.; Bi, H.; Liu, Y.; Fan, Y.; Gao, H.; Wang, Y.; Hou, Z. *J. Mater. Chem.* **2009**, *19*, 8072. (c) Peng, T.; Yang, Y.; Liu, Y.; Ma, D.; Hou, Z.; Wang, Y. *Chem. Commun.* **2011**, 3150. (d) Peng, T.; Yang, Y.; Bi, H.; Liu, Y.; Ma, D.; Hou, Z.; Wang, Y. *J. Mater. Chem.* **2011**, *21*, 3551.

(7) Martyn, P. C. *Dalton Trans.* **2006**, *8*, 985.

(8) Recent reviews: (a) Edelmann, F. T. *Adv. Organomet. Chem.* **2008**, *57*, 184. (b) Zhang, W.-X.; Hou, Z. *Org. Biomol. Chem.* **2008**, *6*, 1693.

(9) (a) Bailey, P. J.; Pace, S. *Coord. Chem. Rev.* **2001**, *214*, 91. (b) Duncan, A. P.; Mullins, S. M.; Arnold, J.; Bergman, R. G. *Organometallics* **2001**, *20*, 1808. (c) Mullins, S. M.; Duncan, A. P.; Bergman, R. G.; Arnold, J. *Inorg. Chem.* **2001**, *40*, 6952. (d) Bazinet, P.; Wood, D.; Yap, G. P. A.; Richeson, D. S. *Inorg. Chem.* **2003**, *42*, 6225. (e) Soria, D. B.; Grundy, J.; Coles, M. P.; Hitchcock, P. B. *J. Organomet. Chem.* **2005**, *690*, 2278. (f) Wilder, C. B.; Reitfort, L. L.; Abboud, K. A.; McElwee-White, L. *Inorg. Chem.* **2006**, *45*, 263. (g) Rische, D.; Baunemann, A.; Winter, M.; Fischer, R. A. *Inorg. Chem.* **2006**, *45*, 269.

(10) (a) Rohde, J.-U.; Matthew, R. K.; Lee, W.-T. *Inorg. Chem.* **2008**, *47*, 11461. (b) Gantzel, P.; Walsh, P. J. *Inorg. Chem.* **1998**, *37*, 3450. (c) Hauber, S.-O.; Niemeyer, M. *Inorg, Chem.* **2005**, *44*, 8644. (d) Rohde, J.-U.; Lee, W.-T. *J. Am. Chem. Soc.* **2009**, *131*, 9162.

(11) Graces, F. O.; Dedeian, K.; Keder, N. L.; Watts, R. J. *Acta Crystallogr.* **1993**, *C49*, 1117.

(12) (a) Colombo, M. G.; Hauser, A.; Gudel, H. U. *Inorg. Chem.* **1993**, *32*, 3088. (b) Colombo, M. G.; Brunold, T. C.; Riedener, T.; Gudel, H. U. *Inorg. Chem.* **1994**, *33*, 545.

(13) Ohsawa, Y.; Sprouse, S.; King, K. A.; De Armond, M. K.; Hanck, K. W.; Watts, R. J. *J. Phys. Chem.* **1987**, *91*, 1047.

(14) (a) Wang, Y.; Herron, N.; Grushin, V. V.; LeCloux, D.; Petrov, V. *Appl. Phys. Lett.* **2001**, *79*, 449. (b) Garces, F. O.; King, K. A.; Watts, R. J. *Inorg. Chem.* **1988**, *27*, 3464.

(15) (a) Brooks, J.; Babayan, Y.; Lamansky, S.; Djurovich, P. I.; Tsyba, I.; Bau, R.; Thompson, M. E. *Inorg. Chem.* **2002**, *41*, 3055. (b) Hay, P. J. *J. Phys. Chem. A* **2002**, *106*, 1634. (c) Kulikova, M.; Balashev, K. P.; Kvam, P. I.; Songstad, J. *Russ. J. Gen. Chem.* **2000**, *70*, 163.

(16) In a control experiment, the lithium guanidinate Li{(-N^{i}Pr)$_2$CN(C$_6$H$_4$)S} showed an oxidation potential at 0.65 V (see Figure S12 in the Supporting Information), which is similar to the second oxidation potential of **5** (0.75 V). However, its PL (λ_{max} = 515 nm) was rather weak (see Figure S2 in the Supporting Information).

(17) (a) Chia, Y. C.; Lu, H. C.; Wu, C. G.; Chen, J. G.; Ho, K. C. *Adv. Funct. Mater.* **2007**, *17*, 29. (b) Pommerehne, J.; Vestweber, H.; Guss, W.; Mahrt, R. F.; Bassler, H.; Porsch, M.; Daub, J. *Adv. Mater.* **1995**, *7*, 551. (c) Liu, Y.; Ma, H.; Jen, A. K.-Y. *Chem. Mater.* **1999**, *11*, 27.

(18) (a) Nishida, J.-I.; Echizen, H.; Iwata, T.; Yamashita, Y. *Chem. Lett.* **2005**, *34*, 1378. (b) Ono, K.; Joho, M.; Saito, K.; Tomura, M.; Matsushita, Y.; Naka, S.; Okada, H.; Onnagawa, H. *Eur. J. Inorg. Chem.* **2006**, *18*, 3676. (c) Adachi, C.; Tsutsui, T.; Saito, S. *Appl. Phys. Lett.* **1989**, *55*, 1489.

(19) (a) Zhu, Y.; Kulkarni, A. P.; Jenekhe, S. A. *Chem. Mater.* **2005**, *17*, 5225. (b) Kulkarni, A. P.; Tonzola, C. J.; Babel, A.; Jenekhe, S. A. *Chem. Mater.* **2004**, *16*, 4556. (c) Shirota, Y. *J. Mater. Chem.* **2005**, *15*, 75. (d) Oh, J.-J.; Kim, K.-W.; Kim, M.-S.; Kwon, T.-W.; Park, D.-K.; Cho, S.-J.; Woo, H.-S. *Appl. Phys. Lett.* **2006**, *89*, 073504. (e) Lai, R. Y.; Kong, X.; Jenekhe, A. A.; Bard, A. J. *J. Am. Chem. Soc.* **2003**, *125*, 12631.

(20) (a) Liu, Q.-D.; Mudadu, S. M.; Thummel, R.; Tao, W.; Wang, S. *Adv. Funct. Mater.* **2005**, *15*, 143. (b) Qiang, F.; Bing, X.; Biao, J.; Haitao, F.; Xiaoyao, C.; Amin, C. *Chem. Commun.* **2005**, 1468. (c) Qianqian, L.; Jianhua, Z.; Junwu, C.; Zijun, L.; Jingui, Q.; Zhen, L.; Yong, C. *J. Phys. Chem. B* **2009**, *113*, 5816.

(21) (a) Brunner, K.; Van Dijken, A.; Borner, H.; Bastiaansen, J. J. A. M.; Kiggen, N. M. M.; Langeveld, B. M. W. *J. Am. Chem. Soc.* **2004**, *126*, 6035. (b) Thomas, K. R. J.; Lin, H.; Tao, Y.-T.; Ko, C.-W. *J. Am. Chem. Soc.* **2001**, *123*, 9404. (c) Morin, J.-F.; Drolet, N.; Tao, Y.; Leclerc, M. *Chem. Mater.* **2004**, *16*, 4619.

(22) (a) Jason, D. S.; Alon, A. G.; Michael, S. L.; Jingjing, W.; Sara, P.; Richard, R.; Stefan, B.; George, G. M. *J. Am. Chem. Soc.* **2004**, *126*, 2763. (b) Tao, Y.; Qiang, W.; Chuluo, Y.; Kai, Z.; Qi, W.; Taotao, Z.; Jingui, Q.; Dongge, M. J. *Mater. Chem* **2008**, *18*, 4091. (c) Wang, J.; Jiang, Y. D.; Yu, J. S.; Lou, S. L.; Lin, H. *Appl. Phys. Lett.* **2007**, *91*, 131105.

(23) Nonoyama, M. *Bull. Chem. Soc. Jpn.* **1974**, *47*, 767.

(24) *SMART Software Users Guide*, version 4.21; Bruker AXS, Inc.: Madison, WI, 1997.

(25) *SAINT PLUS*, version 6.02; Bruker AXS, Inc.: Madison, WI, 1999.

(26) Sheldrick, G. M. *SADABS*; Bruker AXS, Inc.: Madison, WI, 1998.

(27) Sheldrick, G. M. *SHELXTL*, version 5.1; Bruker AXS, Inc.: Madison, WI, 1998.

(28) Runge, E.; Gross, E. K. U. *Phys. Rev. Lett.* **1984**, *52*, 997.

(29) Becke, A. D. *J. Chem. Phys.* **1993**, *98*, 5648.

(30) (a) Hay, P. J.; Wadt, W. R. *J. Chem. Phys.* **1985**, *82*, 270. (b) Hay, P. J.; Wadt, W. R. *J. Chem. Phys.* **1985**, *82*, 299.

(31) (a) Casida, M. E.; Jamorski, C.; Casida, K. C.; Salahub, D. R. *J. Chem. Phys.* **1998**, *108*, 4439. (b) Stratmann, R. E.; Scuseria, G. E.;

Frisch, M. J. *J. Chem. Phys.* **1998**, *109*, 8218. (c) Matsuzawa, N. N.; Ishitani, A.; Dixon, D. A.; Uda, T. *J. Phys. Chem. A* **2001**, *105*, 4953.
(32) (a) Barone, V.; Cossi, M.; Tomasi, J. *J. Chem. Phys.* **1997**, *107*, 3210. (b) Cossi, M.; Scalmani, G.; Rega, N.; Barone, V. *J. Chem. Phys.* **2002**, *117*, 43.
(33) (a) Monat, J. E.; Rodriguez, J. H.; McCusker, J. K. *J. Phys. Chem. A* **2002**, *106*, 7399. (b) Zhou, X.; Zhang, H. X.; Pan, Q. J.; Xia, B. H.; Tang, A. C. *J. Phys. Chem. A* **2005**, *109*, 8809. (c) Liu, T.; Xia, B. H.; Zhou, X.; Zhang, H. X.; Pan, Q. J.; Gao, J. S. *Organometallics* **2007**, *26*, 143. (d) Liu, T.; Zhang, H. X.; Xia, B. H. *J. Phys. Chem. A* **2007**, *111*, 8724.
(34) Frisch, M. J.; Trucks, G. W.; Schlegel, H. B.; Scuseria, G. E.; Robb, M. A.; Cheeseman, J. R.; Montgomery, J. A.; Vreven, T.; Kudin, K. N.; Burant, J. C.; Millam, J. M.; Iyengar, S. S.; Tomasi, J.; Barone, V.; Mennucci, B.; Cossi, M.; Scalmani, G.; Rega, N.; Petersson, G. A.; Nakatsuji, H.; Hada, M.; Ehara, M.; Toyota, K.; Fukuda, R.; Hasegawa, J.; Ishida, M.; Nakajima, T.; Honda, Y.; Kitao, O.; Nakai, H.; Klene, M.; Li, X.; Knox, J. E.; Hratchian, H. P.; Cross, J. B.; Adamo, C.; Jaramillo, J.; Gomperts, R.; Stratmann, R. E.; Yazyev, O.; Austin, A. J.; Cammi, R.; Pomelli, C.; Ochterski, J. W.; Ayala, P. Y.; Morokuma, K.; Voth, G. A.; Salvador, P.; Dannenberg, J. J.; Zakrzewski, V. G.; Dapprich, S.; Daniels, A. D.; Strain, M. C.; Farkas, O.; Malick, D. K.; Rabuck, A. D.; Raghavachari, K.; Foresman, J. B.; Ortiz, J. V.; Cui, Q.; Baboul, A. G.; Clifford, S.; Cioslowski, J.; Stefanov, B. B.; Liu, G.; Liashenko, A.; Piskorz, P.; Komaromi, I.; Martin, R. L.; Fox, D. J.; Keith, T.; Al-Laham, M. A.; Peng, C. Y.; Nanayakkara, A.; Challacombe, M.; Gill, P. M. W.; Johnson, B.; Chen, W.; Wong, M. W.; Gonzalez, C.; Pople, J. A. *Gaussian 03*, revision C.02; Gaussian, Inc.: Pittsburgh, PA, 2003.